Analyst

Accepted Manuscript

ROYAL SOCIETY OF CHEMISTRY

www.rsc.org/analyst

Vibrational Spectroscopic Methods for Cytology and Cellular Research

Graeme Clemens[1*], James R. Hands[1], Konrad M. Dorling[1,2], Matthew J. Baker[1,3*]

[1]Centre for Materials Science, Division of Chemistry, University of Central Lancashire, Preston, Lancashire, PR1 2HE, UK

[2]Agilent Technologies, 5500 Lakeside, Cheadle, Cheshire, SK8 3GR, UK

[3]WestCHEM, Department of Pure and Applied Chemistry, University of Strathclyde, 295 Cathedral Street, Glasgow, UK, G1 1XL

Corresponding Authors: gclemens@uclan.ac.uk and matthew.baker@strath.ac.uk / mjbaker@uclan.ac.uk (@ChemistryBaker)

Abstract

The use of vibrational spectroscopy, FTIR and Raman, for cytology and cellular research has the potential to revolutionise the approach to cellular analysis. Vibrational spectroscopy is non-destructive, simple to operate and provides direct information. Importantly it does not require expensive exogenous labels that may affect the chemistry of the cell under analysis. In addition, the advent of spectroscopic microscopes provides the ability to image cells and acquire spectra with a subcellular resolution. This introductory review focuses on recent developments within this fast paced field and highlights potential for the future use of FTIR and Raman spectroscopy. We particularly focus on the development of live cell research and the new technologies and methodologies that have enabled this.

Introduction

Robert Hooke FRS, an English natural philosopher, architect and polymath, was the first person to coin the word 'cell'. The word cell derives from the Old French *celle* or Latin *cella* meaning "storeroom or chamber" [1]. The publication of Hooke's *Micrographia* in the 17th Century [2,3] and his observation of microscopic cell walls in cork tissue provided the basis of what was to become cell theory. Cell theory states that all eukaryotic organisms are composed of cells, and that cells are the smallest independent units of life [4]. Since the discovery of their fundamental importance in the biological sciences, cells have become the focus of much research. Major techniques for the analysis of cells currently rely upon the use of exogenous fluorescent labels. However, there are number of issues with these techniques, including time consuming sample preparation, cost, and the addition of such labels can cause potentially harmful effects, modifying the surface chemistry of a cell, thus causing stress and damaging live cells [5,6]. There has been great interest in the use of vibrational

spectroscopy, Fourier Transform Infrared (FTIR) and Raman, for the analysis of cellular samples due to simple sample preparation, the acquisition of direct information and with the advent of spectroscopic microscopes, the ability to image cells and acquire spectra with a subcellular resolution. In order not to reproduce the aims of other reviews and to focus on recent research the authors will point readers to excellent literature reviews throughout. The increasing interest in FTIR and Raman can be seen in Figure 1 showing the results of a bibliometric analysis.

Raman scattering is an inelastic process that occurs when a molecule enters a virtual excited state due to an incident photon, then falls back to a higher or lower vibrational energy with the accompanying release of a new photon. The energy transfer is proportional to a specific vibrational mode of the molecule and the changes in energy between the incident and released photon is associated with specific vibrations of molecular bonds [7]. Raman spectroscopy is a vibrational spectroscopy technique used to collect unique information on the chemical constituents of a sample; the electric field of the incident light interacts with the molecules in the sample through the polarizability of these molecules. Polarizability is related to the ability of electronic clouds surrounding the moleulce to interact with an electric field [8]. Thus, this technique provides biochemical information about a sample, including conformation and concentrations of constituents with a level of detail that is informed by the instrument and need of application [9]. Table 1 shows the spectral information with tentative assignments acquired for Raman cellular spectra. Raman has shown to be an excellent technique for biological / biomedical analyses possible of detecting and discriminating different types of cancer from tissue and biofluids [10, 11] and many different types of bacteria [12]. The authors point the reader to an informative review by Ellis *et al.* for further information on the use of Raman as a diagnostic tool [13]. However, only a small percentage of photons (one in 10^6 and 10^8 photons) will undergo Raman scattering. Because of this low efficiency, Raman spectroscopy has only become useful since the combination of high intensity continuous wave lasers and sensitive detectors [14-17]. Even with the use of this combination in the instrumental setup, long spectral acquisition times are needed to achieve adequate S/N [16]. Like IR spectroscopy, Raman spectroscopy is a label free technique with the potential for non-invasive and non-destructive discrimination of cells. However, this is reliant on the monochromatic laser sources used. A number of studies have shown that lasers can damage cells through either photochemical, photothermal or photomechanical stress (photodamage), such as the work of Chan *et al.* [17].

Infrared radiation causes vibrations of bonds of molecules within the sample that absorbs it. The wavelength of the incident IR radiation absorbed depends on the atoms involved and the strength of any intermolecular interactions. In order to be infrared active and absorb infrared energy the

molecular vibration must induce a change in the molecular dipole moment. Each molecule can have a different spectrum; in essence the IR spectrum is a fingerprint of the sample. Spectra of biomolecules allow measurement of complex molecular vibrational modes that contain valuable information on any biochemical changes within the sample. Infrared spectroscopy is quick cost-effective (no expensive reagents necessary), simple to operate, reagent free and requires simple sample preparation. Table 2 shows the spectral information with tentative assignments for FTIR cellular spectra. FTIR has also been shown as a useful tool in the biomedical sphere capable of discriminating many types of cancer [18], model cell lines [19] and bacteria [20]. Due to the increased information content of the mid-IR spectral region, this region has seen an increase in its use for cellular analysis. As such this review will focus on mid-IR spectroscopy. For a brief explanation of specifics of the techniques discussed in this review please see Table 3.

IR and Raman are complementary spectroscopic techniques with some molecular vibrations being favoured to one technique rather than the other i.e. a molecular vibration which gives a strong Raman signal usually produces a weak IR signal and vice-versa. For example, vibrations of polar bonds and asymmetric molecules tend to absorb strongly for IR spectroscopy, whereas these molecules produce poor intensities for Raman spectroscopy, and symmetric and non-polar are more suited for Raman investigations [15]. Although Raman and IR spectroscopy are complementary spectroscopic techniques, they require different photophysical processes [15]. This results in both Raman and IR having some advantages over one another. One of the advantages of Raman spectroscopy is that, unlike FTIR, the technique does not have a problem with water absorption when investigating aqueous solutions. This is due to polar molecules, such as water, producing relatively weak Raman signals, therefore, Raman spectroscopy is currently a more suitable analytical method to probe and investigate live cells spectroscopically. In the case of biological samples, another advantage of Raman is that the spectra recorded often exhibit sharp bands in the spectrum, whereas an IR spectrum often contains broad absorption bands thus, no need to deconvolve a spectral band to reveal overlapped molecular information. Raman microspectroscopy also offers much increased spatial resolution over its counterpart [21]. Furthermore, Raman scattering can be employed in the UV, visible or near IR regions of the electromagnetic spectrum, meaning that typical materials can be used for the fabrication of microfluidic devices to be coupled with Raman spectroscopy.

Since their combination with optical microscopes, FTIR and Raman spectroscopy have become popular analytical methods for the characterisation of single cells. Although monitoring of cells using FTIR and Raman microspectroscopy offers a snapshot of cells biochemistry and have become

relatively widely used, new research is still uncovering and overcoming factors associated with the fundamental interaction of light with biological samples and several phenomena influence the spectrum. The main phenomena that could influence a cellular spectrum are:

1) Scattering – A measured IR spectrum contains contributions from absorption, reflection and scattering [22]. As cells are comparable in size to the wavelength of mid-infrared radiation they scatter the infrared light directed upon them during FTIR analysis. Therefore, the spectrum will contain information upon the biochemical constituents of a cell as well as its size / morphology. The Gardner group, University of Manchester, have developed a pre-processing algorithm in collaboration with Nofima Mat, Centre for Biospectroscopy, Norway in order to remove this contribution from the spectrum [23]. Another approach to understanding this affect of light interacting with matter has been proposed by a pioneer in the field, Rohit Bhargava, University of Illionois. Prof. Bhargava presents a model based approach to retrieve the true spectral information. As the morphology of the sample (such as spheres or nuclei) affect the spectral properties as well as chemicals present this is important to understand. Bhargava *et al*. have presented an optical physics based approach that predicts the recorded data from PMMA spheres, which are shown to be strongly dependent upon the size of the sphere and instrumental factors, obtains the complete refractive index of the material using data from the sphere and thus the effects of morphology can be removed revealing the shape-independent IR absorption spectrum of the material [24]
2) Electric Free Standing Wave (EFSW) Artefact – There is currently great interest in the Biophotonics field directed towards the recent discovery of the EFSW artefact. An EFSW is present at reflective metallic surfaces due to the interference of the incident and reflected light [25]. This occurs when analysing samples upon reflective low-e surfaces using FTIR. This has the effect of introducing spectral information based upon the thickness of your sample rather than the biochemical content and could lead to mis-identification or discrimination particularly during single cell analysis when there is a large difference in the height profile of a cell. However, recent work by Cao *et al.* [26] demonstrated no difference in classification between transflection and transmission FTIR measurements on dried cellular monolayers when transforming data to 2^{nd} derivative spectra before classification using pattern recognition algorithms.
3) Fluorescence – occurs when an electronically excited molecule decays back to the ground state spontaneously, emitting radiation at a frequency characteristic of the transition between the excited and ground states [27]. The probability of Raman scattering (cross-

section) is much lower [28] than fluorescence, therefore, fluorescence can swamp a Raman spectrum. The use of near infrared (NIR) lasers to irradiate the sample reduces this phenomenon; as wavelengths in this region do not typically induce the electronic transitions in cellular chromophores that contribute to fluorescence. Also below 250 nm no fluorescence interference exists. In addition, the use of immersion Raman spectroscopy for both live cell and *in vitro* tissue specimens on CaF_2 substrate, observed an improvement of spectral quality, sample stability and the reduction of spectral background [29]. Also, Surface Enhanced Raman Spectroscopy (SERS) can have a fluorescence enhancing effect [30].

FTIR and Raman spectroscopy are frequently performed on fixed monolayers of cells, effectively recording spectra from a dead sample. Sample preparation is a key step in enabling vibrational spectroscopy to achieve its potential in this field. Sample preparation methods can have a significant impact on the interpretation of spectra for their biochemical relevance and on the spatial distribution of biomolecules in imaging studies [31]. The authors point the readers to an excellent resource by Lyng *et al.* on this subject [31]. In summary, for cellular analysis, a study using FTIR spectroscopy investigated different chemical fixation methods for the analysis of adipocytes found that the spectra are able to be discriminated based upon the fixation method utilised [32] and a study using Raman spectroscopy comparing fixation methods to live cells showed that levels of fixation were found to be cell line dependent [33]. Therefore, even standardising the fixation method utilised for an experiment could confound vibrational experimentation by the influence of external agents. The use of chemical fixation affects the vibrational modes of lipid, protein, nucleic acid and carbohydrate moieties. However, it has been concluded that formalin fixation [33] generates a spectrum that has the highest similarity to that of a live cell. When comparing air dried, dessicated, and formalin fixed samples using Raman spectroscopy formalin fixation produced the weakest spectrum but the most consistent with air drying providing slightly more consistency over desiccation [34]. Fixed samples do not represent a cells natural environment nor does if offer a practical real life model for cell screening. As such, there has been an increasing move in the field to use 3D spheroid cultures, that more accurately represent the microenvironment of cells, and live cell analysis.

A major consideration for the analysis of vibrational spectra when directed towards detection and discrimination is data analysis including pre-processing and multivariate analysis. The Martin group, University of Lancaster, have provided an in-depth review and perspective of the future of extracting biological information with computational analysis from spectra and the authors point the reader to this resource [35].

This review will discuss pioneering work performed in the use of vibrational spectroscopy for cytology and cellular research as well as provide possibilities that will enable these powerful techniques to achieve their potential. This review is structured such that FTIR, ATR-FTIR and spontaneous Raman are discussed first in each section followed by specialist techniques (by subheading). Explanations of the techniques discussed in this review can be found in Table 3.

Prokaryotic Cell Research

Microorganisms such as bacteria perform a multitude of roles in the environment that are beneficial (e.g. detoxify or attenuate pollutants) and essential for life on planet earth to exist but they can also cause life-threatening illnesses (e.g. Plague). Microorganisms are the most abundant and diverse forms of life on Earth [36]. As an example of their diversity members of the *Bacillus* species can be used for production of riboflavin [37], a major additive of animal feedstock's and a human food and pharmaceuticals, and as the causative agent of Anthrax. In addition, the rise of protein drugs, biopharmaceutical processing and biocatalysis, has produced a massive industry with microorganisms at its core. As such the analysis, identification and discrimination of microorganisms, in particular bacteria, is an ever developing area of interest and one within which vibrational spectroscopy has become a useful tool.

In a review on the use of vibrational spectroscopy directed towards microbiological investigations it would be neglectful to not include any of a number of studies performed by the groups of Prof. Dr Dieter Naumann, Robert-Koch Institute, Berlin, Germany, Dr Gerwin Puppels, University of Twente, Netherlands and River Diagnostics and Prof. Roy Goodacre, University of Manchester, Manchester, UK. The pioneering work of Prof. Dr Naumann showed the use of FTIR combined with computer based pattern recognition algorithms for discriminating and identifying 36 clinical isolates of *Staphylococcus aureus* and 24 of *Streptococcus faecalis* demonstrating that, for the first time, FTIR provides classification similar to conventional classification schemes [38] and that infrared signals recorded from microorganisms are highly specific fingerprint-like patterns [39]. Naumann *et al.* utilised pre-selected windows based upon their discriminatory power, namely, 3000 – 2800 cm^{-1} (dominated by $–CH_3$, $>CH_2$ and ≡CH), 1800 – 1500 cm^{-1} (information from amide I and II vibrations), 1500 – 1200 cm^{-1} (information from proteins, fatty acids and phosphates), 1500 – 1400 cm^{-1} (dominated by bending vibrations $–CH_3$, $>CH_2$ and ≡CH) and 900 – 700 cm^{-1} (the true fingerprint area of spectral patterns yet unassigned to functional groups or cellular components). Since the development of the Raman microscope by Puppels *et al.* [40] Raman microspectroscopy has been shown possible of discriminating bacterial strains such as the study by Goodacre *et al.* which exemplified the use of Raman to differentiate 59 bacterial isolates of urinary tract infection (UTI)

bacteria [41]. Goodacre *et al.* highlighted the beneficial use of Raman to analyse single cells. Generally a Raman microbial spectrum can be defined by characteristic C-H stretching in the range of 2700 -3100 cm^{-1}, C-H deformation band around 1450 cm^{-1}, amide I ~1660 cm^{-1}, amide III ~1250 cm^{-1} and well documented peaks for RNA/DNA nucleotide base-ring vibrations and Phenylalanine [42]. Following these fundamental studies many groups have furthered the use of Raman and FTIR for the classification of bacterial strains. The authors point the reader to excellent reviews on the use of Raman and FTIR in microbiology [42-43].

The major drivers for the interest in the bacterial spectrum came from food security / processing, defence and healthcare. These are still major drivers today and have expanded to include the addition of biopharmaceuticals and bioprocessing, building upon previous work and with newly developed methodologies, Raman and FTIR spectroscopic analysis are enabling these industries and research fields.

For the defence, healthcare and food security domains major interests lie in the identification of pathogenic bacteria. In particular for defence, the identification of *Bacillus anthracis*, the causative agent of Anthrax, bacteria such as Methicillin resistant *Staphylococcus aureus* and *Staphylococcus aureus* in medicine and food security. Many studies in this area have shown the ability of Raman and FTIR to discriminate different bacterial strains [44-46] and River Diagnostics have a commercial instrument specifically designed instrument (SpectraCell RA ® Bacterial Strain Analyzer) for this purpose. These studies have shown the usefulness of vibrational spectroscopy for rapid identification of pure cultures. In order to develop this technology to enable its use there is a critical need to develop portable / handheld instruments that are capable of *in situ* classification, further develop methodologies capable of identifying bacteria within the environment in the presence of complex matrices, increased specificity to allow for pure bacterial spectra from mixtures to be collected, increased sensitivity to enable the detection of bacterium at lower concentration levels to allow for early monitoring and the development of tools and techniques to provide further information on the bacterium. This review will assess current research towards this aim.

Recent work has shown the use of Raman spectroscopy to identify *Brucella* within the complex matrix of milk [47] providing a detection capability that does not rely upon the cultivation of pure bacteria prior to analysis. Meisel *et al.* spiked milk with samples of *Brucella, Escherichia, Ochrobactrum, Pseudomonas* and *Yersinia* and achieved sensitivities and specificities of identification ranging from 83 – 100 % with the *Brucella* spectra differentiated by higher intensities of the DNA, proteins (1440 cm^{-1}) and lipids and fatty acids. This study showed that bacteria can be identified within 2 h without the need for cultivation to create a pure bacterial culture. Nicolaou and

Goodacre [48] focused on the use of FTIR for the rapid and quantitative detection of microbial spoilage in milk. Using ATR-FTIR and High Throughput (HT) FTIR they profiled milk at eight hourly time intervals up to 104 h. Interestingly, the major difference between the two techniques was the absence of CH_x vibrations in the 2900 and 2800 cm^{-1} spectral range for ATR-FTIR spectra, corresponding to the acyl chain of fatty acids. It is thought that due to the micellular globules of the lipid in milks the penetration depth of the ATR-FTIR evanescent wave meant that these chemical were not analysed whereas HT-FTIR uses the transmission sampling mode of FTIR, also the ATR spectra were collected from liquid samples whilst the HT-FTIR were dried. Both techniques were able to acquire a metabolic snapshot and quantify the microbial load of milk samples within 30 s and with little sample preparation thus, showing FTIR as a viable rapid method for bacteria detection and quantification. A study by Ellis *et al.* on horizontal ATR – FTIR (HATR-FTIR) exemplifies the ability of spectroscopy to assess microbial load directly from the matrix, in this case meat spoilage [44]. Combining HATR-FTIR with machine learning methods highlights the region between 1088 and 1096 cm^{-1} as a salient range for the identification of chicken spoilage. The peak absorbancies at 1088 and 1240 cm^{-1} increased at the point of spoilage onset and can be attributed to C-N stretching of amines. These peaks can be attributable to free amino acids which indicate proteolysis. It is known that spoilage in meat is frequently associated with the utilization of amino acids by microorganisms leading to the production of free amino acids [49]. Using fibre evanescent wave spectroscopy (FEWS) to collect infrared spectra Brandily *et al.* [50] discriminated between endogenous flora, *Listeria, Salmonella*, and *Staphylococcus* on sausage meat, minced meat and unpasteurised cheese when combined with principal component analysis (PCA) and logistic-partial least squares (PLS). Argryi *et al.* [51] compared the use of Raman and FTIR spectroscopy for the prediction of meat spoilage, collecting time series spectra from minced beef samples stored in aerobic and modified atmosphere packaging. It was shown that FTIR based models performed slightly better, this combined with rapid spectral collection makes it an advantageous technique, in predicting the microbial counts compared to the Raman models and in general for both techniques, better predictions were obtained for TVC (total viable counts), LAB (lactic acid bacteria), and *Enterobacteriaceae* and demonstrated that both FTIR and Raman can be used reliably and accurately for the assessment of meat spoilage. It is advantageous to be able to detect whether a cell is dead or alive as well, as currently the use of common methods for cell identification in a food sample such as Enzyme linked Immunosorbent assay (ELISA) does not provide that discrimination and can lead to a false positive if dead cells are present. A study using FTIR [52] showed the use of FTIR spectroscopy to differentiate live, dead and treated *E. coli* cells. Using Canonical Variate Analysis (CVA) it was possible to discriminate 100% live, 100 % dead and 99% dead: 1% live without any misclassification,

the authors followed this analysis using a Partial Least Squares (PLS) model to obtain the quantification of live *E. coli* in the presence of dead cells showing a linear correlation and an R^2 of 0.996 when spectral regions from the sections identified by Naumann were included, speeding up the process of quantification of live bacteria over methods such as fluorescence microscopy.

For the defence arena there is a requirement to identify and differentiate pathogenic bacteria *in situ* in order to enable a suitable, and correct, response to be deployed whilst maintaining operational tempo. Bacterial warfare agents (BWAs) are defined as any organism or toxin found in nature that can be used to incapacity, kill or otherwise impede an adversary [53]. General interest is in the bacterium *Bacillus anthracis*. Trials, by the UK government, on Gruinard Island has shown that *B. Anthracis* remains viable in the environment for many years, annual soil samples from 1948 – 1968 and again in 1982 and 1979 contained viable spores [54]. Central to the persistence of *B. Anthracis* is its ability to form an endospore that is resistant to environmental pressures, however, it should be noted that some bacteria, considered to be BWAs, do not form spores and exist solely in a vegetative form. In the case of Gruinard Island and terrorist attacks, BWAs will be present in a mixture with other environmental flora and fauna. Samuels *et al.* [55] have used FTIR to classify category A and category B bacteria (US national Institute of Allergy and Infectious Disease classifications of priority pathogens) showing the ability to differentiate between *B. Anthracis* spores and vegetative cells as well as classification of *Yersinia pestis*, *Francisella tularensis* and *Brucella abortus.* Recent research by McIntosh *et al.* examined the effect of environmental conditioning on the FTIR spectrum of bacterial biological warfare stimulants [56]. Following discrimination of a subset of bacterial biowarfare simulants, this study cycled the temperature and humidity of the bacteria moving from 30 – 44 °C with an associated change in humidity from 40 – 14 %, these conditions were held for 8 hours and then reversed to recreate the diurnal cycle of a hot dry climate. Spectral collection was then undertaken from the environmentally conditioned bacteria to discover if current models could differentiate environmentally conditioned bacteria from bacteria collected under optimum laboratory conditions. The study concluded that it is important to take into account the pattern recognition algorithm used for spectral interrogation as support vector machine(s) (SVMs) was shown possible of identification, but a principal component – discriminant function analysis (PC-DFA) was not; a linear discriminant boundary was not sufficient for the data. Future analysis and further understanding of the variant and invariant features of the vibrational biological spectrum would prove valuable for a BWA spectroscopic detection system. Raman spectroscopy has been shown capable of discriminating many different strains of pathogenic bacteria and very adept at analysing dipicolonic acid, a biomarker of sporulation. Many groups have examined DPA as a marker for BWA spores [57]. A recent study by Hermelink *et al.* [58] has shown the ability of confocal

Raman spectroscopy to probe the heterogeneity at the single cell level. Discriminating the difference between the vegetative cell and sporulated cell population of *Bacillus cereus* (Figure 2). When required *B. cereus* can synthesis Poly-β-hydroxybutryic acid (PHB) and accumulate it in intracellular granules. PHB has a significant C=O stretching vibration at 1726 cm^{-1} and sporulating cells can be indicated by the CaDPA Raman spectrum with bands at 825, 1018, 1451 and 1574 cm^{-1}.

Surface Enhanced Raman Scattering (SERS)

Surface Enhanced Raman Scattering (SERS) is a powerful fingerprinting technique [13,30,234] that is proving valuable in the bacterial research. During SERS analysis the Raman signal of a molecule is enhanced by orders of magnitude compared to normal Raman when in close proximity / adsorption on a roughened metal surface, a colloidal solution of metal nanoparticles (normally Au or Ag) or a roughened metal electrode. An incredibly active field of SERS has shown its use for the identification of BWAs as the enhanced detection seen when using SERS allows the culturing step to be removed enabling rapid detection in the field. The longevity of BWAs is mainly due to the ability to create resistant endospores and the dipicolonic acid (DPA) biomarker is easily distinguishable using SERS. However, not all endospores are lethal and natural environmental spores will be present. There is a requirement for SERS to be able to distinguish multiple cellular identities and this could be achieved through combining SERS with multivariate analysis algorithms and multiplexed detection regimes. Jarvis *et al.* [57] used an aggregated silver colloid substrate to differentiate between closely related *Bacillus* strains with SERS combined with PC-DFA. Interestingly the authors showed a difference in reproducibility between Gram-positive bacteria and Gram-negative bacteria, which was assigned to the uniformity of the Gram-positive cell wall. The ability to differentiate spores of *B. subtillus* from vegetative cells of the same strain was shown to be due to DPA. This study has therefore shown the ability to fingerprint different strains of *Bacillus* and identify sporulated from vegetative cells from the same species. SERS shows excellent promise as a rapid tool for BWA detection and based upon on Calcium dipicolinate (CaDPA) as a spore differentiation tool. Zhang *et al.* [59] used an extraction procedure and silver film over nanosphere substrates to detect a LOD of ~2.6 x 10^3 spores, below the anthrax infectious dies of 10^4 spores. However, this process does require the spores to be handled / processed, with the development of possible microfluidic separation procedures this could be an interesting fieldable application. An alternative method to enhance the specificity of the SERS approach, to discriminate between closely related bacteria, is using peptide functionalised SERS active substrates [60]. This methodology was able to bind *B. Anthracis*-Sterne for detection via SERS but did not show affinity for the closely related B*. subtillus* and *B. cereus* species. The SERS substrates were functionalised with a *B. anthracis*-Sterne specific peptide; each *Bacillus* species was

allowed to bind to the protein for 15 minutes and then washed to remove any unbound spores before the introduction of acetic acid. Only the *B. anthracis*-Sterne sample produced a DPA spectrum characterised by peaks at 821, 1014, 1391, 1446 and 1537 cm^{-1}, which have been assigned to a ring CC bend, an out-of plane CH bend, the symmetric pyridine ring stretch, a symmetric OCO stretch, a symmetric ring CH bend, and an asymmetric OCO stretch, respectively [60]. Another example of enabling specific detection is shown by recent work from Dr Faulds, University of Strathclyde, in the form of multiplexed SERS. Faulds has shown the use of multiplexed SERS for the detection of five oligonculeotides in a mixed sample using different SERS dyes and excitation wavelengths, this was performed without the need for multivariate analysis [61]. Expanding this work into the healthcare domain Gracie *et al.* [62] have simultaneously detected and quantified three bacterial meningitis pathogens. Gracie *et al.* designed an assay to detect *S. pneumonia, N. meningitides* and *H. influenza* when coupled with three different reporter dyes (FAM, TAMRA and Cy3) coupled with exact synthetic DNA sequences linked to each pathogen. By exploiting the different dye spectra observed and using PLS it was possible to quantify the amount of pathogen present in a multiplexed samples. Using the 1650 cm^{-1} peak (*S. pneumomaniae* linked to the TAMRA reporter dye), 646 cm^{-1} (*N. meningitides* linked to the FAM reporter dye) and 1586 cm^{-1} (*H. influenza* linked to the Cy3 reporter dye) produced limits of detection of between 21.7 pM – 99.5 pM with R^2 values between 0.9905 and 0.9938 proving reproducible and quantifiable SERS opening up the possibility of rapid multiplexed detection of multiple pathogens in a reproducible and portable manner. Figure 3 shows the multiplexed spectrum and responses from single bacteria reproduced from Gracie *et al.* [62].

Confocal Raman Microspectroscopy

Confocal Raman microspectroscopy uses a spatial filter to ensure that the Raman signal is controlled and originates from a defined space in 3 dimensions (x,y and z) [238-240]. This allows the user to selectively analyse samples with an approximate 1 µm voxel resolution. An interesting use of Raman to provide information on single cells is the use of confocal Raman microspectroscopy, capturing a single cell spectrum and removing spectral contributions from neighbouring cellular matter. Schuster *et al.* [63] analysed single cells of the anaerobic bacterium *Clostridium beijerinckii*. This technique can analyse cells from culture down to the smallest size of ~1.5 by 0.7 µm with the detection limit of the single cell being ~1 pg (10^{-12}g). Productive biotechnological process depend upon the optimum performance of the utilised catalyst, using 3D Raman confocal microspectroscopy, the authors demonstrated a technique that could assess the heterogeneity within a cell population with excellent resolution. Confocal Raman in combination with laser

tweezers has been shown capable of identifying bacteria. Xie *et al.* [64] used laser tweezers and hierarchical cluster analysis (HCA) to discriminate between six bacterial species (*B. cereus, E.coli, E. Faecalis, E. aerogenes, S. pyrogene* and *S. salivarius*) using a synchronised culture to ensure the bacterial cells are at the same point in their life cycle and are generally the same size produced clearly distinguishable groupings with PCA based upon relative intensities of peaks at different positions, for instance the Raman intensity of 783 to that of 1004 cm^{-1} for *E. aerogenes* is approx. 0.85 whilst for all other species is close to 1. The bacterial growth stage depends on many factor such as nutrition, pH etc. and in the natural environment most bacteria will lie in an unsynchronised stationary state as well as random growth phases. This study analysed the ability to discriminate bacteria in the environmental stationary state Another study showed the use of laser tweezers and confocal Raman to identify single bacterial spores in aqueous solutions [65]. The advantage of these processes open up the potential of combining Raman spectroscopy with a flow cytometric set up for the rapid, reagentless identification of bacteria without fixing and without the application of exogenous fluorescent labels. Other developments have shown the use of Raman for the analysis of live bacterial cells. Zhou *et al.* [66] have combined the use of atomic force microscopy (AFM) and Raman microspectroscopy to profile *Pseudomonas putida*. The combination of these two techniques allows the collection of biomechanical / biophysical information as well as biochemical information and in this case allowed for the investigation of the adhesions force of the flagella and microscpectroscopic evaluation of the biochemical structural components. This combination can provide new information to further develop our understanding of cellular processes and their inherent properties, for instance, the increased virulence of certain *Bacillus* species. Further work has shown the ability to profile biofilms enabling the identification and discrimination of the different species contained within the biofilm [67] using bands at 988, 1446 and 1529 cm^{-1} attributable to crystalline calcium phosphate, algal lipid and algal pigments respectively. This study profiled the structure of a biofilm in the natural environment without interfering with the sensitive microbiota. Enabling the collection of direct information from the natural environment will allow for the advantages of biofilms (wastewater clarification and one stage deammonification) to be further studied in ways that were previously not possible surpassing previous studies.

Coherent Anti-Stokes Raman Scattering (CARS) and Stimulated Raman Scattering (SRS)

Coherent anti-Stokes Raman scattering (CARS) and stimulated Raman scattering (SRS) microscopies [244-251] are label-free and chemically specific imaging techniques that are emerging as very useful methods for rapid imaging cells and tissues based on the intrinsic vibrational spectroscopy of their molecular components. CARS is a four-wave mixing process using two lasers (pump and Stokes),

when the frequency difference between these lasers is tuned to the frequency of Raman active molecular vibrations an enhanced anti-Stokes Raman signal is observed, this is a non-linear effect, the signal is generated at the point of laser focus, allowing for point by point 3D imaging. SRS, again uses two lasers, when the signal matches a molecular vibration enhancement of the vibrational transition occurs, however unlike CARS, there is no effect when the frequency difference does not mat a vibrational resonance allow for a non-resonant background signal. There are numerous advantages to using CARS for cellular and biomedical imaging. It allows for low excitation powers and fast scanning rates, and has high capabilities for three dimensional sectioning [68]. However, as successful as CARS biomedical research has been, especially in showing its capabilities for visualising lipid distributions in live cells [69-70], technological advances have shown that SRS microscopy and imaging research is becoming more common. SRS has its advantages over CARS for biomedical imaging, enabling the possibility of more quantitative chemical imaging due to the absence of unwanted nonresonant background relating to added undistorted spectroscopic information available similar to that obtained from conventional spontaneous Raman. With all the benefits of nonlinear optical microscopy opening the way for possibilities of intraoperative imaging, more and more studies are being done to improve on the accuracy and effectiveness of cancer surgery. The Xie group at Harvard University, USA, have been paramount to the developmental studies of SRS in the biomedical imaging world.

The authors would like to draw focus here to two excellent research papers. The first is by Cheng and Xie, outlining the instrumentation, theory and applications of CARS microscopy, where historical developments of the technique have led CARS microscopy to being a powerful tool for the vibrational imaging of unstained samples [68]. The second, by Evans and Xie, investigates the developments of CARS microscopy specifically in biology and medicine, citing the technique's relevance to clinical applications [71]. In bacterial identification CARS has been shown to be highly sensitive for the detection of bacterial endospores, in fact, via a single-shot [72]. This study showed the ability of CARS to analyse 10^4 *Bacillus subtillus* spores collecting Raman spectra from 1100 – 2000 cm^{-1}. This region has previously been used for discrimination of many different bacterial strains showing that CARS is a suitable technique for the rapid identification of biological hazards. In a study comparing CARS and spontaneous Raman spectroscopy for the analysis of *B. subtillus* spores, it was found that CARS spectroscopy is at least two orders of magnitude more efficient than Raman and can lead to 100 times faster remotes sensing and detection of biohazards [73]. Further developments in CARS have led to FAST (femtosecond adaptive spectroscopic techniques) CARS, which Scully *et al.* [74] have proposed will enable the fingerprinting of bacterial spores speculating

on the use of FAST CARS for the stand-off detection of airborne particles. If possible, this would provide a real time, sensitive and specific technique for biohazard assessment.

Raman Activated Cell Ejection (RACE)

Raman Activated Cell Ejection (RACE) uses a microfocused laser beam to eject the required cells from a sample based upon their Raman spectrum. A recent study by Wang and co-workers demonstrates that, for the first time, a single cell Raman spectrum (SCRS) can be obtained with just a 0.1 second acquisition time [75]. A compelling aspect of the study reported by Wang *et al.* is the rapid timeframe at which a SCRS is obtained. The Raman system used was optimised in three ways to improve Raman spectral quality; 1) shortening the Raman light path, 2) utilizing a low noise and sensitive EMCCD for Raman signal detection and 3) increasing the incidence laser power. This system was shown capable of discriminating *S. sanguinis, S. mutans, P. gingivalis, . faecalis,* and *A. viscosus*. SCRS from *Escherichia coli* (*E. coli*) were collected with an acquisition time of 0.1 second, signal-to-noise ratio (SNR) of 4, and exhibits similar spectral quality to that obtained from the old non-optimised system which has a SNR of 3.92. *E. coli* grown in 2 mediums supplemented by either 5 g/L ^{13}C-glucose or 98 atom % ^{15} N-NH_4Cl, thus labelled with ^{13}C and ^{15}N, was successfully discriminated between when using the new rapid system. The spectral bands shifted to a lower wavenumber due to the incorporation of ^{13}C and ^{15}N atoms into the cells. Principal component analysis (PCA) successfully discriminated between the normal cells (^{12}C and ^{14}N) from those grown in ^{13}C and ^{15}N media.

Wang *et al*. rapidly screened 20 randomly selected *E. coli* cells. Among those cells selected, 11 were identified as ^{13}C-cells because of the significant shift in the phenylalanine band from 1003 to 697 cm^{-1}. To identify cells in complex microbial communities Raman activated cell ejection (RACE) assisted by laser induced forward transfer (LIFT) was used. An interesting approach to sorting single cells. LIFT occurs by focusing a pulsed laser through a transparent substrate onto a light-absorbing layer (e.g. water). Forward momentum occurs when the thin film of water surrounding the cell evaporates, allowing for the isolation of the desired cell. ^{13}C-*E. coli* cells and bacteria from natural groundwater (assumed to be ^{12}C) were rapidly Raman screened. The ^{13}C-labelled cells were identified based on the phenylalanine band shift, previously discussed. The rapid SCRS approach is novel and it highlights and draws emphasis to the future potential of RACE (assisted by LIFT) as a tool of choice for personalised medicine, cytology and cellular research [75].

Eukaryotic Cell Research

Cells are implicated in all diseases. In terms of cancer, a normal cell is transformed into a cancerous one when normal cell cycle checkpoints are disrupted through gene and protein alteration. This alteration to the cell cycle results in aggressive, uncontrolled proliferation and cellular growth that can lead to tumour formation [76-77]. According to Cancer Research UK [78], more than 331,000 people in the UK were diagnosed with cancer in 2011, over 900 people a day. With more than a third of cancers being diagnosed in people over 75, and people living much longer, this figure is set to rise. Therefore, new technologies to aid rapid early diagnosis would be the most beneficial [79]. In instances where diagnosis of cancer often requires invasive biopsy examinations, cancer diagnosis through cytological examination of a small number of cells has obvious advantages. Current methods used for cytological examination of cells are performed by trained cytopathologists as well as immunohistochemical staining / flow cytometric analysis. However, although highly trained, cytopathologists are only human and there is the potential for subjective analysis as well as examinations being time consuming [80]. One current method of screening cells is known as the Pap test, which is a screening method for cervical cancer, involving the visual examination and diagnosis of chemically stained cells using an optical microscope. Cervical disease is classified through the use of the 2-tier Bathesda system for Pap smears (low and high grade squamous intraepithelial lesions) and the 3-tier cervical intraepithelial neoplasia system for surgical samples (CIN I, II, III). However, studies have shown that the test is prone to human error, with the overall accuracy being relatively low [77, 78-80] and the sensitivities and specificities of the test depending on a number of subjective factors [79]. A false positive result of the test would result in a patient undergoing unnecessary treatment and anxiety. On the other hand, a false negative result is a more harrowing scenario where a patient can go undiagnosed, adding to the chance of carcinoma progression. Therefore, there is a real need to develop new diagnostic methods to aid cytopathologists perform cytological examinations for the early detection of disease. Such methods would be rapid, require little sample preparation, be relatively cheap, non-destructive and cellular diagnosis should not be subjective.

Since the first demonstration of FTIR microspectroscopy (FTIR-MS) being used to provide sub cellular resolution on single cells by Jamin *et al.* in the late 1990s [81], there has been growing interest in the use of IR spectroscopy in the field of cellular diagnosis. The coupling of optical microscopes with FTIR spectrometers allowed microspectroscopic measurements achieving spatial resolutions appropriate for the investigation of single cells [82]. As well as this, subcellular spectral information recorded from cells could now be combined with visually images, therefore, allowing detailed histopathological correlation between cell spectra and disease stage [79-82]. Because spectral profiles of single cells can often be similar, FTIR-MS is predominately coupled with multivariate approaches to capture subtle, but significant, biochemical differences between different cell spectra.

Such multivariate techniques allow spectra to be grouped according to spectral similarities between recorded spectra thus, highlighting the potential for non-subjective diagnosis/discrimination of cell spectra. Early pioneers of the field include N. Jamin [81], H. Y. Holman [83-85], B. R. Wood and D. McNaughton [86-88], M. Diem [89-98] and M. A. Cohenford and colleagues [99].

Early studies investigating eukaryotic cells with IR spectroscopy used exfoliated cells, smears and cell pellets. However, the cellular constituents of these cellular samples contained many different cell types, which can have an effect on the IR spectrum recorded. Other variations, such as inflammation, metaplasia, the ratio of non-dividing to dividing cells and the overall divisional activity of the cells, as well as cervical debris attained from scrapes, will also dramatically affect the spectrum recorded. All described factors will confound spectral analysis results. Therefore, it became apparent that cellular diagnosis based on such samples would be problematic, with the possibility of discrimination between samples, but not based on the spectral changes between normal and diseased cells [78, 100]. This showed the importance of monitoring the molecular changes of single cells, so as to understand the spectroscopic signatures of cells going through normal life cycle phases (cell cycle phases, differentiation and maturation), as well as necrosis/apoptosis and inflammation, in order to be able to distinguish abnormal molecular variations of diseased cells. Early studies required the high brightness of synchrotron radiation (SR) coupled with an FTIR-M spectrometer (SR-FTIR-MS) to achieve the necessary S/N to record spectra from individual eukaryotic cells [81-85]. One such study [83-85] combined SR-FTIR-MS with Fluorescent Activated Cell Sorting (FACS), to investigate the spectral changes of individual living human cells in different phases of the cell cycle (G1, S and M phases) and cell death. Spectral results of average spectra showed clear differences when comparing the recorded cell spectra from cells in the different phases. Cells in the S phase of the cell cycle showing markedly increased intensity from absorption bands associated with DNA/RNA, when compared to spectra recorded from cells in the G1 phase. With DNA being replicated throughout the S phase of the cell cycle, the increase in nucleic acid content in cells in the S phase were seen as a reasonable assumption. A study by the Diem group [101] also investigated the IR profiles of single proliferating ML-1 cells using both PCA and Artificial Neural Networks (ANN's). Analysis results showed that cell spectra recorded from cells in G1 and G2 cell cycle phases exhibited systematic variations in the amide I and II vibrations, and could be separated into distinct clusters using PCA. The clustering of cell spectra recorded from S phase cells was much more difficult though using PCA, with S phase cell spectra exhibited large heterogeneity. However, studies that investigated the molecular changes of cells undergoing different phases of the cell cycle using IR spectroscopy, did not take into consideration the inherent

change in morphology of proliferating cells. These analysis results will have been, to some extent, contaminated by scattering dispersions [102].

Biological cells and their nuclei/organelles are of a size and shape that will scatter mid-infrared radiation strongly when recording individual cell spectra in air. This scattering distortion of the source beam results in a broad sinusoidal oscillation of the baseline and a significant derivative-like distortion on the high wavenumber side of the amide I band from recorded cell spectra, severely affecting both the intensity and position of the amide I band in the spectrum [81, 103]. Early studies in the field had noticed large spectral variations from recorded single cell spectra, with one study observing large spectral heterogeneity in exfoliated epithelial cells that should be divisionally inactive thus, relatively homogeneous. The fact that two near identical cells can produce quite different IR signals was concerning considering the potential use of FTIR-MS for determining cell phenotypes and states of cell health [104]. This cell spectra heterogeneity is now known to be a result of Resonant Mie scattering (RMieS) [81, 103]. Recently, the RMieS-EMSC correction algorithm has been derived, which enables the RMieS component of the spectrum to be calculated and removed from the measured spectrum, leaving only the pure absorption spectrum of the cell [81]. The RMieS-EMSC has been successfully used on a number of recent studies using FTIR-MS to interrogate single cells [105-108]. Transforming spectra to second derivatives and the use of the EMSC correction algorithm can be sufficient in the removing Mie scattering contributions from spectra, however, these processing methods do not model the so called dispersion artefact, which results from the varying refractive index from in the cell relative to the background [79]. Therefore, studies not using the RMieS-EMSC correction algorithm must be cautious when interpreting spectral differences from amide and carbonyl ester absorption bands.

Earlier studies investigated the molecular changes of cells in different phases of the cell cycle showed structural changes to the amide I band to be significant [83-85]. However, without correcting for RMieS, one cannot be fully sure if the amide I structural variations are a result of a molecular difference between the cell spectra recorded from the different phases, or a morphological change (different shape and size), due to cells in one phase of the cell cycle having increased RMieS, when compared to another. A recent study by the Jimenez *et al*. [102] investigated the spectroscopic changes of Caki-2 cells progressing through the cell cycle with the use of RMieS-EMSC algorithm, the aim being to unambiguously assign the spectral features of spectra in each phase. Spectra were recorded from cells in the G1, S and G2/M cell cycle phases and SVMs was used as the classification algorithm. The study showed that cellular features, such as the size and shape of cells in the different proliferation stages, promoted characteristic distortion of the recorded spectra,

and interestingly, the spectral analysis of the uncorrected spectra produced higher classification accuracy than RMieS-EMSC corrected. However, only RMieS-EMSC corrected spectra contain just biochemical information, raw uncorrected spectra contains both the cell cycle dependant biochemical features and the RMieS distortion, which is related to morphological features of the cell in the different phases. Therefore, if the aim of the study is to understand the biochemical differences between cell cycle phases, RMieS must be removed from recorded cell spectra [102].

In 2003, a study by Gazi and co-workers showed that IR spectra recorded from prostate cell lines, derived from different metastatic sites, could be distinguished [109]. Results showed that the 1030 and 1080 cm^{-1} (1030/1080 cm^{-1}) peak area ratio, associated to glycogen and phosphate vibrations respectively, suggested a potential method for the discrimination of benign and malignant cells. Benign cells showing a higher ratio value, whereas malignant cell types a lower. The decrease in glycogen level from malignant cells, when compared to normal prostate epithelial cells, was suggested to be due to the higher metabolic activity of the cells thus, an increase in glycolysis to fuel the energy requirements of the highly proliferating malignant cells. A study in 2006, suggested a role for FTIR-MS in the screening cancerous cells found in urine. A study of the accuracy of urinary cytology in daily practice found that the diagnostic sensitivity of high grade transitional cell neoplasms was roughly 79%, whereas the sensitivity in low grade transitional cell neoplasms was confirmed to be roughly 26% [100]. Bird *et al*. presented a correlation between the spectral patterns recorded from cells and the cytological identification of normal cell types found in human urine (visual examination of PAP stained cells). PCA was able to group cell spectra recorded from glycogen free and glycogen rich squamous cells, as well as urothelial (transitional) epithelial cells, along the PC3 scores axis. Highlighting the potential of IR spectroscopy for the objective screening of cancerous cells found in biological matrices like urine [110].

A recent study investigated the application of FTIR-MS to assess the effect of chemical stains on single cell spectra [111] The study suggests a role for FTIR-MS to help pathologists better understand suspicious cells through examining whether haematoxylin (H&E) and Pap staining affects single cell spectra, and if IR recorded spectra from the lung cancer cells can be discriminated from their normal counterparts. SR-FTIR-MS was used to record spectral data collection from individual cells. The high brightness of synchrotron produced IR radiation allows small spatial resolutions to be probed with good S/N, whereas conventional thermal sources perform admirably when large apertures are employed, as the majority of light reaches the detector, however, when apertures are closed down to 30 x 30 µm or smaller, thermal source struggle to achieve an effective SNR. The increase in brightness from synchrotron produced IR radiation coming from IR light being highly collimated into

small spatial regions without large losses in light intensity. Results showed that both chemical stains induced a spectroscopic change from the cells, with both stains mainly affecting the bands in the spectrum associated with lipids, the amide II band and the spectral band situated at ~1305 cm^{-1}. The lipid changes represented decreases in intensities from the CH2 stretching modes at 2850/2920 cm-1 respectively, and the carbonyl C=O stretching mode of phospholipid structures. These decreases was said to be a direct result of the ethanol washes used in both staining procedures, removing phospholipids and other membrane lipids from cells. The spectral changes from the amide II and the ~1305 cm-1 band were confirmed in the study as being from addition of haematoxylin when using both stains. Nethertheless, spectra recorded from already stained lung cancer cells could be discriminated from their normal counterparts (also stained). This showed that the addition of such stains to cells has not added to the heterogeneous intra class variance of spectra recorded, or masked the biochemical differences between the cancerous lung cells and their normal counterparts. Typically, when combining FTIR spectroscopy with pathologist examinations of stained cells, FTIR spectra must be recorded first and the optical examination happens afterwards. However, there are a number of drawbacks with this methodology. Therefore, this study highlights a more practical and simpler methodology, [111] which has the potential to make it to the clinical practise as an additional diagnostic tool in pathology.

FTIR-MS has also been shown to be useful for the screening of cervical cancer cells [78, 99, 112-118]. In a study making use of FTIR-MS, 53 subjects were used to test the ability of the Pap smear test and IR spectroscopy to classify normal and abnormal cells, results were tested against the findings of Colposcopists. The Pap smear test achieved an overall classification of 43%, whereas the classification of IR recorded spectra achieved a rate of 72% [115]. An early study using FTIR-MS [78, 99, 115] showed cancerous sample spectra to have a 1026 cm^{-1}/amide II ratio that was less than half that of the normal group spectra, highlighting the glycogen absorption band as a potential diagnostic marker. The ratio decreasing for spectra recorded from normal, dysplasia and cancer respectively [78, 99]. However, a later study [112], using ATR IR spectroscopy (ATR-IRS) to record cell spectra, showed spectral bands primarily associated protein macromolecular structures (amide I band) and absorption bands located in the 1500- 1200 cm^{-1} spectral range to be key discriminative band features. Both PCA and Principal Component (PC) fed Linear Discriminant Analysis (PC-LDA) results showed normal, low grade and high grade exfoliated cervical cancerous cells could be separated. Inter-category variance was associated to protein and DNA conformational changes, whereas the glycogen band strongly influenced intra-category variance. Authors suggest differences in sampling techniques for glycogen levels being an important contributor to intra-category variance. A recent

study using IR spectroscopy proposed new features of cervical cell spectra, suitable for the discrimination of both normal and abnormal cervical cells. Some of the purposed features include the area under the spectrum between 1500-1800 cm^{-1}, area under the spectrum between 1000-1200 cm^{-1}, area under the spectrum between 950-1800cm^{-1} and height of the slope of the band between 1650 and 1550 cm^{-1}. Extracted features can be used as inputs for classification algorithms, such as neural networks. The new cervical cell features were extracted from recorded spectra and fed into the multilayered perceptrons (MLP) network, trained using Levenberg-Marquardt Backpropogation (trainlm) algorithm, recording a classification accuracy of 97.3% when classifying normal from abnormal cervical cells [116]. A further study by Jusman and colleagues [117] again extracted FTIR characteristics from recorded cell spectra (Peak-corrected area based features' extraction (PCABFE)) to classify normal, LSIL (Low grade intra-epithelial squamous lesion), and HSIL (high grade intra-epithelial squamous lesion) cervical pre-cancerous cells; distinguished according to the Bethesda classification. Analysis by Hybrid Multilayered Perceptron (HMLP) network showed 97.4%, 100%, 95.2%, 0.0%, and 4.8% of accuracy, sensitivity, specificity, negative, and false positive values, respectively [117]. Another recent study by the Martin group [118], also made use of extracting features and tested the performance of four different classifiers to classifying normal, low and high cell spectra. The top 25 most significant features from the recorded spectra were selected using eClass, these were subsequently used as inputs to test the performance of four different classifier algorithms; SVMs, K-nearest neighbour (k-NN), artificial neural networks (ANNs) and eClass. Results showed that feature extraction fed SVM to produce the best classification results from the study. However, the authors rightly state that SVM has the potential to overfit, plus, the computational complexity of the SVMs requires large CPU memory requirements. On the other hand, the self-learning classifier, eClass, exhibited robust predictive power in a user-friendly fashion when compared to the other classifiers. The study highlights the unique characteristics of eClass, which show distinct advantages of over commonly used classification algorithms (adaptive, no parameters to be user-tuned, and interpretable). Such properties highlight the potential for feature extraction fed eClass classification as an alternative to SVMs and other commonly used classifiers [118].

HPV DNA has been detected in 99.7% of cervical cancer cases, correlating the HPV infection with the disease. Analysis results of a study performed by Schubert *et al*. show that HPV infected cells could be discriminated from non-infected, based on changes to the amide I and II absorption bands. Therefore, a possible early diagnostic marker of disease cells [79, 100]. Although the combination of the Pap test and HPV DNA testing has been shown to offer an improvement in the sensitivity of

classifying abnormal cells, tracking the course of the disease in women would not be cost effective using such testing [79, 100]. Therefore, with little consumables needed, IR spectroscopy may be a more desirable technique for discriminating HPV infected cells. Another study [119] explored the potential of using FTIR-MS to correlate spectroscopic features with HPV infection levels and expression levels of the p16INK4A biomarker. The p16INK4A expression level has been shown to be a proven and reliable biochemical marker of cervical immunocytochemical dysplasia and was found to mark all grades of squamous and glandular lesions of the cervix using methods. Confocal fluorescence microscopy and flow cytometry, revealed p16INK4A expression to be correlated with HPV infection levels in cervical cancer cell lines thus, confirming the biomarker as a diagnostic marker for cervical cancer. Using FTIR-MS coupled with PLS analysis, the expression level of p16INK4A could be predicted based on the spectral fingerprint recorded, demonstrating the diagnostic potential of spectroscopic techniques. Analysis results revealed spectral differences between bands associated with nucleic acid, lipid and proteins between cell lines with varying HPV copy number. Interestingly, nucleic acid peak intensities were showed to have increasing tendencies and lipid peak intensities decreasing with increasing HPV copy number. Although their correlation was non-linear with HPV copy number, their dependence on p16INK4A levels was found to be close to linear.

A number of recent studies have also shown IR spectroscopy to be useful tool for the diagnosis of leukaemia cells [120], cells infected with the poliovirus infection [121], prion infection [122], human papilloma virus (HPV) [100], human breast cancer cells with estrogen receptor expressed and not expressed [123], and cancer stem cells [124]. Didonna *et al.* [122] used SR-FTIR-MS to investigate the biochemical perturbations undergone by prion infected mouse hypothalamic GT1-1 cells, at the cellular and subcellular level. Results from the study showed that HCA could be used to discriminate spectra recorded from infected and non-infected cells. Both the optical examination and AFM analysis of the cells showed the different cell types to be similar in size, shape and cellular volume. As a result of this, it was believed that both GT1-1 and ScGT1-1 cell spectra were roughly proportional to the concentration of the cellular constituent, therefore, no need to normalize spectra before comparison. Without normalisation, a decrease in total cellular protein content was seen when comparing prion infected spectra; results were validated by other techniques. The decrease in overall protein content for infected cells was also seen when protein chemical maps of the different cell types were produced. As well as this, phospholipid and lipid chemical maps of single cells showed the phospholipid distribution of infected cells to be quite different from GT1-1 cells. This study exemplifies the use of SR-FTIR-MS as a powerful tool monitor the macromolecular

alterations of a cell at the sub-cellular level, without the need of adding potentially harmful biomarkers, therefore, aiding our understanding of cellular disease; SR providing adequate spatial resolution for sub-cellular spatial resolution.

Chemotherapy agents have been so instrumental in the successful treatment of cancers in many patients over the years. However, some cancers are very difficult to control, and some will come back. Therefore, new research in this field is helping to improve the quality of people living with cancer. One such area of research is exploring the effects of smaller concentrations of chemotherapy drugs [125]. A study by Sulé-Suso *et al*. [126] showed that spectra recorded from gemcitabine treated lung cancer cells revealed biochemical differences, which were dependant on the dose of gemcitabine added to the cells, *in vitro*. Gemcitabine being known to bind DNA in its triphosphate form, which causes the arrest of cell proliferation, accumulating cells in the G1 phase of the cell cycle [127]. The data showed an increase in intensity from the 1080 cm-1 spectral band and the 1080 cm−1/1050 cm−1 ratio when gemcitabine was introduced to the cancerous cells. This increased as the dose increased to the lethal dose 75 (LD75) for A549 lung cancer cells, and between the LD50 and LD75 for the Calu-1 lung cancer cells. At these doses the ratio reached a plateau phase. This study showed that IR spectroscopy can be used as a tool to assess the usefulness of chemotherapy drugs on cancerous cell lines, therefore, highlighting the potential of FTIR-MS to shed light on the exact dose at which a chemotherapy agent becomes cytotoxic, rather than just inhibiting cellular growth. Helping in the understanding of what is the minimal dose of chemotherapy agent necessary to kill cancerous cells. Further work by Sulé-Suso and colleagues [127] used IR spectroscopy to investigate the sub-toxic doses of gemcitabine on (0.1 to 100 nM for 24, 48 and 72 h) on non-small cell lung cancer cells (Calu-1). Drug concentrations of 0.1, 1, 10 and 100 nM induced 5, 23, 82 and 95% of cell growth inhibition respectively without inducing cell death. Cell viability results showed that 95-100% of cells were viable at all doses and time points after drug introduction; cell viability was assessed using the Trypan blue exclusion test. The Kruskal-Wallis test was used distinguish the most discriminant spectral ranges in the spectral dataset before HCA cluster analysis. Spectral ranges included 3088–3049, 2980–2947, 2937–2909, 2873–2845 and 1137–1106 cm^{-1}. Cluster analysis results showed that the recorded spectra could be clearly classified into two main groups, one group containing spectra from cells exhibiting weak and moderate proliferation rate (control cells and cell treated with 0.1 and 1 nM concentrations) and another group containing spectra from cells representing high proliferation growth rate inhibition (cells treated with 10 and 100 nM concentrations). Bands associated with protein and RNA molecules are seen to increase in gemcitabine treated cells. The work demonstrates that spectral fingerprints of gemcitabine treated

lung cancer cells, arresting in the G1 phase, can be distinguished using IR spectroscopy. Spectra were recorded using both SR-FTIR-MS and a High–Throughput-Screening EXTension (HYSXY) device coupled to a Tensor-27 FT-IR spectrometer, which has the capability of recording automatic measurements of samples (spectra recorded in transmission mode) using a 96 well plate (cells seeded onto the surface of a silicon-based plate), highlighting the potential of FTIR as a high throughput instrument for rapid measurements.

Other recent studies have also used IR spectroscopy to investigate the molecular effects of chemotherapy agents on cell populations. One using ATR-FTIR spectroscopy to ascertain the molecular effects of polyphenolic compounds, which are an important part of the human diet, on cancerous cells [128], Gasper *et al*. [129] investigating the effect of Ouabin (anti-cancer drug that is intended to enter clinical trials soon) and other chemically similar cardiotonic compounds on human prostate cancer cells [130], and Flower and colleagues [105] used SR-FTIR-MS to investigate the different mode of action of a recently synthesised cytotoxic di-gold(I) organometallic complex (KF0101) on ovarian cells (A2780 cell line). The molecular effects of KF0101 were compared to the spectroscopic actions of cisplatin, methotrexate, paclitaxel and 5-fluorouracil on A2780 cells.

Research into the molecular alterations of cells help shed light on the molecular mechanisms involved certain cell events, such as transformation to disease state and cell death. A number of studies by the Martin group have used IR spectroscopy to investigate molecular alteration of the MCF-7 breast cancer cell line [131-136]. The most recent study by the group [136] looked into benzo[a]pyrene-induced cell cycle associated alterations using ATR-FT-IRS. Benzo[a]pyrene (B[a]P) is a pro-mutagenic and pro-carcinogenic contaminant derived from tobacco smoke, car exhaust fumes, industrial wastes and food products, and can bind/activate the aryl hydrocarbon receptor (Ahr), and when activated, is a key component of the B[a]P-induced target genes' expression response. The induced responses are associated with the modification of genes and proteins involved with a number of biological mechanisms, including the cell cycle and apoptosis. The studies aim was to see if spectra recorded using ATR-FTIR spectroscopy, coupled with PC-LDA multivariate analysis, could detect the low (10-9 M) and high dose (10-6 M) related cell cycle effects of B[a]P on the MCF-7 cells; concentrated in S or G0/G1 cell cycle phases. B[a]P treated cells were compared with vehicle only (DMSO treated) treated cells to determine the magnitude of biochemical alterations. Results successfully showed clear spectral differences between S and G0/G1 cells, treated with both drug concentrations and the vehicle (control cells). The biochemical differences between cells in the same cell cycle phase after treatment with both low and high dose, when compared to the control cells,

show changes in biochemical action with both drug concentrations inducing different actions. Humans are rarely exposed to high concentrations of such environmental contaminants. However, some humans may well be exposed to low doses but over a long period of time. With IR spectroscopy being able to capture minor biochemical changes in a cell signal, this study reveals that even low doses (10-9 M) can have a molecular effect on cell populations, without actually causing cell death. Many age-related diseases may well involve subtle alterations of surviving cells through low dose exposures over many years. Therefore IR spectroscopy has potential to study long term effects of low dose contaminants on healthy cells.

Some of the studies mentioned have used FTIR-MS spectral imaging to record chemical images of samples (Figure 4). Chemical images can be produced through either sequential mapping (often using SR), or through the use of a Focal Plane Array (FPA) detector. Spectral analysis through classification algorithms or multivariate analysis can either be performed on the data contained within the recorded images, or on cellular spectral information which has been extracted from images. With chemical images having subcellular spatial resolutions and covering a large area, this has allowed chemical images to be compared with stained images. FPA detectors allow the simultaneous recording of thousands of spectra (128 x 128 FPA pixel detector collects 16384 spectra at a time) [137], resulting in the much faster image acquisition times when compared to chemical images produced through sequential mapping. An early study by Lasch and colleagues [90] reporting a 360:1 data collection time advantage for FPA spectral imaging compared to sequential mapping. FPA detectors are now in regular use in benchtop FTIR-MS instruments thus, increasing the number of studies using FPA recorded chemical images to extract chemical data from single cells. Because of the speed in which a chemical image can be recorded using an FPA detector, hundreds of single cell spectra can be recorded in a matter of minutes, instead of hours. A study by Filik *et al.* [138] provides an excellent methodology for extracting relevant single cell information from chemical images, see Figure 5.

A number of studies have also suggested that IR spectroscopy could potentially discriminate single cells in a matter minutes. This would be a major advantage considering that the time in which traditional techniques used for cellular analysis take. However, the discrimination of eukaryotic cells using IR spectroscopy will not happen until live cells are interrogated; the sample preparation process of chemically fixing/drying cells is not trivial. Although a small number of early studies investigated the molecular alterations of live cells [183], the majority of studies have involved chemically fixed or dried cells. This is due to there being several limitations imposed by surrounding

cells in aqueous media [139]. However, a number of common fixative methods used to preserve the chemistry of cells for IR measurement have been shown to have issues; notably, a reduction in nucleic acid structure from preserved cell spectra when compared to the spectra recorded from live cells. Authors state that this may be a result of nucleic acid denaturation when chemical fixatives or air drying methods are employed. Therefore, suggesting that only live cell spectra provide reliable information on both DNA and RNA structure. This is in agreement with a study performed in 2011 [140], which showed B-like DNA to be present In hydrated live cell spectra, with an overall shift from B-like DNA to A when cells are dehydrated; subsequent rehydration returning the B-like from again. When in the A conformational DNA state, DNA vibrations are more difficult to detect and distinguish in recorded spectra because of low intensity absorptions and band broadening, whereas the hydrated B-like DNA are more easily observed. Therefore, when DNA may be a marker of interest, investigated hydrated live cells with IR is an advantage. Investigating live hydrated cells has another 2 advantages (i) live cells suspended in aqueous buffer solution represents an environmental state which is close to the *in vivo* conditions of cells (ii) water has a refractive index that is similar to the biological constituents making up a biological cell. Therefore, live cell spectra can be recorded in an aqueous matrix with little, if any, RMieS observed [252,253]

Exciting work by the Fryer group in 2003 highlighted the use of FTIR combined with viable cells in suspension as an optimum methods for cellular analysis, the spectra showed reduced measurement artefacts and facilitate the quantification of cellular biochemical components [141]. In order to record cell spectra from live cells, FTIR-MS can be coupled with a micro-device that is capable of achieving an appropriate water optical thickness. Typically a water barrier of <10 μm is preferred so that water absorption does not mask molecular signatures [142]. Holman *et al.* provide excellent methodologies for the tracking of live cells identifying that the spatial resolution and detection sensitivity can be increased by using a synchrotron source [142]. This early work has enabled a leap forward in the use of synchrotron radiation for live cell experimentation. Interestingly Holman has been able to follow phosphorylation, without the use of labelling which is the current gold standard, on individual cells as they differentiated into nerve cells. The ability to follow intracellular molecular changes in live cells opens up the possibility of tracking new biology more sensitively. This form of functional IR spectromicroscopy has been developed by Quaroni *et al.* showing the ability to follow metabolic processes and driving FTIR forward in order to address key biological questions such as structure-function studies and kinetic processes within single cells and with a subcellular resolution [143].

A number of studies by Vaccari and co-workers [139, 144-146] have demonstrated that good single cell spectra can be recorded from living cells when coupling micro-devices with FTIR-MS, therefore, highlighting the potential for truly non-invasive discrimination of individual cells. Several groups have developed micro-devices in order maintain a suitable water barrier, while preserving the integrity of living cells [148]. These include demountable flow chambers [148-149] and open [149] and closed [139-149] micro fluidic devices [139, 147-149]. However, it should be mentioned that suitable data processing methods are needed in order to correctly account for the over-subtraction of the amide I band [139]. One example of IR spectroscopy being used to monitor molecular changes of live single cells is an experimental study investigating the effect of Arsenic trioxide (As2O3), the primary ingredient in the leukaemia drug Trisenox™, on live HL60 leukaemia cells. Cell spectra were recorded using SR-FTIR-MS and a demountable liquid cell employing CaF_2 windows [149]. Importantly, the study showed that through reducing the sample path length to 9µm, the bending mode vibration of the water was reduced sufficiently so that the amide I absorption peak, situated at ~1650cm−1, could be measured. Live cell spectra were produced from subtraction of an aqueous buffer spectrum (collected in an area of the cell free of cellular material) from a cell plus buffer spectrum. However, live cell spectra showed an undulating baseline in all spectra recorded and was attributed to scattering dispersions. Cell spectra were therefore transformed to second derivatives. Observations after 40 minutes exposure of sodium arsenite (100 mM concentration), showed the PO_2^- content to decrease dramatically, but then increase after 100–120 min exposure, along with other molecular alterations which suggested protein conformational changes as a result of arsenite arsenite treatment. IR measurements were accompanied by the trypan blue exclusion assay, which showing the decrease in the number of cells after treatment [139]. Another recent study investigated the molecular changes of live cells (L929 fibroblast cell line) as thy progressed through the life cycle (G1, S, G2 phases). PCA was successful used to cluster spectra of cells in the life cycle phases. The primary biochemical changes of the cells were attributed to overall concentrations of nucleic acids, proteins and lipids. During the first 10 hours post mitosis (cells in G1 phase), cells were observed to increase in protein and decrease in both lipids and nucleic acids. Between 9-11 hours post mitosis ((S) synthesis phase), cells show an increase in lipid concentration as well as strong DNA contributions, possible due to the duplication of the genome. At 4-6 hours after the synthesis phase (G2 phase), again cell spectra from cells are shown to accumulate protein, while nucleic acid and lipid concentrations decrease. With nucleic acids playing major roles in a cells life cycle, this study shows the advantage of investigating cells in a live state, resolving previously unresolved B-DNA information [151]. Another advantageous factor being the reduced scattering observed from recording cell spectra. This enabled the confident assignment of biochemical

differences between cells in the differing cell cycle phases, without computationally intensive corrections being needed.

With the speed advantage of FPA detectors, studies are now recording chemical images of live cells [152-157,254]. Petibois and colleagues, demonstrating the increased quality of chemical images recorded from single cells when using SR and 32 x 32 pixel elements of a 64 x 64 FPA detector (only 32 x 32 because the inhomogeneous distribution of the SR photon flux does not match the full size of the 64 x 64 FPA detector when using a 36X optical objective), when compared to conventional source (typically Globar); high spatial resolution chemical images being recorded in a few minutes using the high brightness of SR. However, another recent study [156] has shown that live cells can be investigated using an ordinary Globar source through the addition of two CaF_2 lenses (one top and the other on the bottom) to a common transmission liquid cell. Therefore, highlighting that live cell experiments on individual cells is possible when using a Globar source. With not many people having regular access to synchrotron facilities, this could be a significant finding in the field. A previous study by the group showed that the use of a lens (CaF_2), placed on the top of a typical transmission substrate, creates a pseudo hemisphere setup, removing dispersion and refraction of light effects, which causes infrared light to focus with different focal lengths depending on the wavelength of the light [157]. This can occur when samples are sandwiched between infrared windows or placed underneath a layer of liquid. As a consequence, chemical images are obtained but with only a particular wavelengths in focus, while the remaining are defocused. The setup of a pseudo hemisphere corrects the spread of the focus, with the light across the spectral range having the same focal depth. Live cell spectra recorded using the lens setup are of a much better quality than those recorded without [156]. As well as providing better quality spectra, the setup also increases both magnification and spatial resolution when compared to a traditional transmission setup of an FTIR-MS instrument [156-157].

Because water produces strong and broad absorption bands that can overlap biochemically information in live cell IR signal, a recent study suggested an alternative medium of mineral oils for recording spectra from live cells [153]. The study also investigated the viability of adherent epithelial cells maintained in mineral oils for short periods of time, with cells immersed in mineral oil (colorectal and urothelial cancer cells) remaining viable for 2 hours, and recovery into normal culture medium was possible (viability staining performed after recovery into an aqueous environment). Thus, the addition of such oils was not a terminal event. For ATR-IR spectroscopy though, the sampling path length does not depend on sample thickness. Instead, the light penetrates into the sample as an evanescent wave, penetrating into a sample under investigation by

only a few micrometres, thereby reducing the optical path length in water (IR light penetrating only several micrometres beyond the ATR crystal penetrating cells seeded to the crystal surface) [158]. The reduced pathlength allows the recording of molecular information from cells without strong absorptions from the aqueous surroundings, thus, overcoming the difficulty of strong water absorptions obscuring important biochemical information in a live cell spectrum, and reducing the challenge of recording IR information from live cells (Figure 6). The combination of ATR-IR spectroscopy and FPA detectors, ATR-FT-IRMS, has also demonstrated that it possible to record data from live cells at sub-cellular spatial resolution. When an ATR objective is used in a microscope, the spatial resolution is enhanced because of the high refractive index of the ATR reflection element. As a result, enhanced spatial resolution chemical images can be recorded, when compared to images recorded using traditional transmission, transflection and reflection methods, therefore, enabling chemical information to be recorded from the different organelles making up a single cell, ATR-FT-IRMS can then be used as a resource to probe biochemically changes within cells at the sub-cellular level, rivalling information recorded at a synchrotron facility. As well as this, ATR-IRS spectroscopy produces no observable RMieS scattering effects, importantly inferring that single cells can be accurately probed in air without the need to apply a suitable correction algorithm.

Exciting new research from Wood *et al.*, Monash Unviersity, have recently exemplified the use of ATR-FTIR spectroscopy for the detection and importantly the quantification of early stage Malaria parasites [159]. The authors detect infected red blood cells with an absolute detection limit of 0.00001 % parasitemia (<1 parasite / µl ob blood) for cultured early ring stage parasites in a suspensions of normal red blood cells. This study demonstrates the positive aspects of ATR-FTIR (portability, small data file size) for *in situ* analysis. However, currently the instrumentation is limited to single sample analysis, in order for ATR-FTIR to achieve its highlighted potential there is a requirement for a continuous sampling process, most likely via microfluidics, or a multi well ATR-FTIR sampling accessory.

Substrate considerations, for FTIR analysis, are an area of great interest within the field with groups suggesting that the use of low e slides results in the electric free standing wave artefact and that these substrates should not be used and others suggesting that simple pre-processing procedures can still enable accurate diagnostic classifications. The vast difference in price between cheap low e slides and expensive alkali halides, potential high sampling numbers for clinical examinations needs discussing in order to agree the most appropriate substrate to improve data analysis reproducibility and allow vibrational spectroscopy to achieve its potential.

Raman microspectroscopy has emerged as a powerful tool for the biochemical analysis of cells and for envisioning the molecular distribution within cells. As technological advances now allow the achievement of higher spatial resolutions, and more detailed datasets which can be obtained through Raman imaging, more work is focused on live-cell monitoring.

In 1990, Puppels and colleagues were the first to combine Raman spectroscopy with an optical microscope creating Raman microspectroscopy [16]. Early studies by the group exploited the advantages of Raman spectroscopy to record spectra from macromolecules inside a living cell. Confocal Raman microspectroscopy being used to achieve the spatial resolutions and sensitivity needed [160-161] (A confocal arrangement reduces out of focus background signals, while passing through focused Raman signals to the detector thus, improving the SNR [17]. Like IR spectroscopy, Raman spectroscopy coupled with multivariate analysis is able to distinguish cell type based on the biochemical Raman signal recorded. Therefore, a number of studies have used the phenomenon of spontaneous Raman scattering to discriminate different cell types in order to highlight the potential of Raman microspectroscopy for cellular diagnosis. This includes neoplastic and normal hematopoietic cells [162], live and chemically fixed cells at different stages of cervical neoplasia [163] cells undergoing stress (Raman images revealing that the cell nucleus shrinks during early stages of stress) [164], normal and cancerous human lung cells [165] and normal fibroblast cells and Huntington's disease (HD) infected fibroblasts. Raman studies have also been designed to evaluate to the molecular effects of chemotherapy drugs being introduced to cancerous cell populations [166].

As previously mentioned, within a population of cells in culture there will be cells in different points in their cell cycle, which will lead to spectral differences between individual cells from the same population (intrinsic biochemical heterogeneity of each cell culture). This can be thought of as within class variability. In the case of investigating spectra recorded from a number of different cell cultures though, one may also assume that cells growing in cultures of different confluence may also add to the within class variability of the spectra recorded. Averaging cell spectra, either through recording spectra from a population of cells or averaging during processing, effectively reduces the within class variability, however, it is important to understand the spectral signals of inherent within class biochemical variability. A study by Matthews *et al.* [167] investigated the use of Raman microspectroscopy to detect the inherent spectral signals of within class variability within live DU145 human tumour cells, cultured *in vitro*. Cells were detached from culture flasks using trypsin and transferred to a low-fluorescence quartz disc for Raman measurements. Spectra were acquired using a 785 nm laser with a sampling volume which allowed a single Raman acquisition to represent the

spectrum of a single cell. Spectral analysis of cell cultures which have not been synchronised (asynchronous) showed typical cell variability. From 24 to 72 hours after sub-culturing, 50%, 20% and 30% of cells were in the G1, G2 and S phases of the cell cycle, between 72-96 hours an increase in G1 phase and a decrease of both the G2 and S phases was seen and after 96 hours, the G2 content remained constant, the S content decreased and G1 content increased until 168 hours; measured through the use of flow cytometry. PCA and flow cytometry analysis showed that the longer the cells were left in culture, after the initial sub-culture, a steady decrease in proliferation is witnessed (Flow cytometry: steady decrease in S phase cells through time), which correlated to a steady decrease in both nucleic acid and protein content, relative to lipid content as a greater fraction of cells became quiescent (non-proliferating (G0 cell cycle phase)); in agreement with previous studies. Interestingly, the spectral differences along PC2 seemed to correlate with the levels of cell confluency in cultures. Cell cultures steadily increase their confluency until five days after sub-culturing (120 hours), when there is little room left to grow and confluency remains relatively constant (~90%). This is reflected in the PC2 scores plot which showed cell spectra recorded at 24 hours to be situated in the negative region of PC2, cell spectra then steadily became more positive along the PC2 axis until ~120 hours, and then remain fairly constant after 120 hours. This spectral variability is independent to cell cycle progression heterogeneity. The spectral differences from synchronised cell cultures showed a continual increase in net nucleic acid/protein content relative to lipid net content, as the cells progressed from early G1 to G1/S and S cell cycle phases. This study shows that not only cell cycle variability contributes to spectral heterogeneity, but also cell culture confluency. A study by Swain *et al.* [168] also used Raman microspectroscopy, but coupled with an immersion lens to record Raman spectra of live cells in order to characterise the biochemical changes related to different cell cycle phases. Analysis results are in agreement with Matthews, Raman spectral showing relative increases in nucleic acid and protein relative to lipid content for cells changing from the G0/G1 phase to the G2/M cell cycle phase. These studies show the potential of the technique for monitoring distinct and subtle molecular changes to live cells, without the need for exogenously added biomarkers, therefore, improving our understanding of normal cellular functions.

Characterisation of healthy cells and cells undergoing cell death, have also been investigated using Raman microspectroscopy. Pyrgiotakis *et al.* [169] successfully classified Raman signals from healthy cells and cells undergoing necrotic and apoptotic cell death using SVMs. Live cells were investigated using a 785-nm laser beam passed through the 63x water immersion Leica objective. However, although it is important to be able to classify the spectral fingerprints of apoptotic and necrotic cell death, SVMs do not explain the molecular differences as to why the spectra can be identified.

Another study however, showed that cells undergoing cell death showed a decrease in the intensity from the 788 cm^{-1} Raman band associated with the DNA molecule phosphate sugar backbone, an indication of DNA disintegration during cell death. Other spectral differences include decreases in intensity from the 1005 and 1342 cm^{-1} Raman bands, associated with proteins, and increases in relative concentration of lipids (1660 and 1303 cm^{-1} bands). Highlighting the potential of Raman microspectroscopy for monitoring the molecular effects of chemotherapy agents on eukaryotic cells [170].

The current methods used to analyse live single eukaryotic cells are FACS or fluorescent imaging. Both methods require the addition of exogenous fluorescent dyes or markers, which then attach to certain molecules on the surface of cell. However, they all have a limited lifetime, after which they undergo irreversible photobleaching and can no longer be probed. The major concern though, is the potential to alter the function (attachment could modify a cells' surface chemistry), or even damage live cells', potentially compromising their clinical use. Other negative factors with the use of such markers include, their use requiring specific specialist knowledge about the cellular systems that they are used with, analysis results saying little about the molecular variations between disease states, and there only being a limited number cell specific markers that exist; In the case of stem cell investigations, no biomarkers have been found for cardiomyocytes, gastrointestinal stem cells, and corneal stem cells. Other single cell analysis techniques are also said to have problems, including the destruction of cell samples as a result of interrogation [171]. Therefore, there is a real need for non-invasive, non-destructive and label-free techniques for the cellular identification and molecular monitoring of living cells. Both IR and Raman spectroscopy are favourable alternatives methods as they can be non-destructive (depending on the laser wavelength and power for Raman experiments and only true when recording data from live cells when using IR spectroscopy), provide label-free discrimination (grouping single cells' based on their intrinsic molecular composition), have the potential to be very fast and can be combined with microscopes so that visual as well as chemical information can be recorded, therefore, complementing cellular staining assays [171].

DNA flow cytometry analysis is currently used to evaluate the malignancy of a tumour. For this method, single-cell suspensions are prepared, stained with a DNA-binding fluorophore, and analysed by a flow cytometer. This analysis detects the number of chromosomes in a cell, searching for extra chromosomes and an increased percentage of S-phase cells undergoing DNA replication to measure the aggressiveness of the cancer. However, this type of analysis does not give any biochemical information to the molecular changes of the cell, from healthy to diseased. Flow cytometric analysis is a high throughput technology, and needs to analyse approximately 20,000 single cells to attain

enough statistical evidence due to variability observed in cellular samples. In order for vibrational spectroscopy to achieve its potential within a flow cytometric application there is a critical need for increased analysis speed and data processing regimes to extract relevant information to enable the large sample sizes required to be analysed. Additionally, flow cytometric analysis, even with spectroscopic advantages, is not a well suited technique for the analysis of a small number of cells, for example, when investigating the small number of cells produced through exfoliative cytology or biopsies on small tumours [172]. In order to analyse these sample numbers the use of live cell vibrational spectroscopy is ultimately more applicable.

Although IR spectroscopy has been shown to have potential spectroscopic investigations of live cells in an environment close to the natural *in vivo* state of cells', the technique is still in its infancy in this field. This is mainly because of the strong IR absorption of OH vibrations from water molecules. However, with water producing a weak Raman signal, Raman spectroscopy is potentially a more suitable analytical method to probe and investigate live cells.

Autography is a cellular process which intracellular material is conserved autophagosomes, which then fuse with lysomes where their contents is degraded to reusable molecular building blocks such as amino acids. This primarily believed to be survival process, induced by various kinds of stress. The role of autophagy in a numerous physiological responses that are triggered by both healthy and disease mechanisms has raised considerable interest in this cellular process. However, methods used to study autophagy are either invasive or require genetic manipulation. Konorov *et al*. [173] present Raman microspectroscopy as a potential alternative to current methods used to study autography. Live cell spectra were recorded using a water immersion lens with 40x objective to focus the laser beam into a rectangular 3 x 30 µm spot. (Laser was generated with 80mW of 785 nm radiation and Raman acquisition time was 100 s per spectrum) Spectral results suggested that the 718cm-1 Raman band, associated with phospholipids, may be a useful spectral biomarker of an autophagic response to cells being starved (glutamine deprivation inducing autophagy). Starved cells showed an increased intensity from the 718 cm-1 Raman band, with the 718/748 cm-1 spectral ratio (phospholipid to nucleic acid ratio) being a potential spectral marker for monitoring cellular response to starvation.

Detection of molecular changes at the single cell level has great potential for understanding the molecular actions of chemotherapy drugs. Like IR spectroscopy, Raman microspectroscopy has been used to monitor the molecular actions of chemotherapy agents on cells. Initial apoptotic molecular changes occur in the nucleus first. With nuclei and cytoplasm spectra representing very different

signals, one study [174] aimed to assess the molecular changes of HL60/ADR (leukemia cell line), CCRF-CEM (Human T cell lymphoblast-like cell line) and HL60 (a human promyelocytic leukemia cell line) cell nuclei, through detecting time resolved changes to nuclei spectra, in response to Doxorubicin and Vinblastine (chemotherapy agents). The excellent spatial resolution of Raman microspectroscopy allows the spectral monitoring of cell nuclei. When HL60 cells were treated with 80 nM doxorubicin for 16 hours, this had the effect of lowering the intensity of Raman bands (predominately nucleic acid peaks) in the 700-1800 cm^{-1} spectral range. Decreases in spectral intensities were even seen with a concentration as low as 3.2 nM/doxorubicin. This decreases in spectral intensities for cells undergoing apoptosis is in agreement with previous study [175]. However, during the initial stage of the study, Raman spectra recorded from whole single cells were investigated. The spectral analysis results of whole cell spectra produced no significant changes to Raman spectra (recorded from associated with DNA or protein until 48 hours. In contrast, spectra recorded from HL60/ADR cell nuclei (HL60/ADR cells are resistant to doxorubicin) showed no spectral changes to doxorubicin, even at 80 nM. The same thing happened when the cytotoxicity of vinblastine was examined in CCRF-CEM and its drug-resistant derivative, the CEM/VBL cell line. The study also assessed the nuclei spectra recorded from cells predominately arrested in $G_0/G_1$and SS and G_2/M cell cycle phases. Raman spectral results were consistent with G2/M cells containing twice the DNA of the G_0/G_1 cells, Raman peaks representative of nucleic acids (e.g. 728, 782, 1095, 1375,1489, 1578 cm^{-1}) being lower in intensity for nuclei spectra recorded from cells predominately in the G_{0}/G_1 cell cycle phase. This study showed the potential for single cell nuclei Raman micro spectroscopy for cytotoxicity studies, with the nuclear changes in response to cytotoxic agents being seen at lower concentrations an in shorter time spans than conventional cell-based assays. Therefore, showing the potential the technique has in aiding in the selection of appropriate chemotherapy agents for cancer therapy. Interestingly, the study also shows that the investigation of the nuclei may be a much better method for monitoring early cell functions, possible due to cytoplasm signals masking subtle, but key, nucleus molecular changes [174].

Bonnier *et al.* have furthered the use of immersion Raman towards biofluids [176], tissue [177] and live cells [178] from the studies exemplified above. Utilising matrigel as a cell matrix for the growth of live cells, Bonnier *et al*. showed that using matrigel as a matrix produces spectra that are independent of the matrix, providing a better Raman substrate than quartz windows and a more natural environment for the cells on which to grow. This greatly reduces the data analysis requirement and the consistency of the signals obtained for the collagen gels will help to standardise the background removal for Raman datasets recorded from live cells. This opens up that possibility of speeding up the data analysis considerations for Raman live cell imaging and when combined with

instrumental advances such as Swift™ or Streamline™ furthers the application of spontaneous Raman spectroscopy in cytological research.

Because of the high spatial resolution of Raman microspectroscopy (low micrometer scale), it has been used to probe subcellular components of cells. In a study by Krafft and colleagues, Raman chemical maps (acquired with a 1 µm step size) were recorded of freeze dried human astrocytoma cells and living human embryonic lung epithelial fibroblasts/human osteogenic sarcoma cells in medium. From the Raman spectral maps recorded, the nucleus, organelles and the cell could be localised using PCA (gray scaled score plot images of PC1 and PC2 displayed). Therefore, instead of Raman peaks of interest being displayed as an intensity map, an intensity map was displayed based on the each spectrums PCA score. Interesting the study showed that the spectral features of the subcellular components were more pronounced for cells in medium. This was presumed to be a direct result of spectra recorded from cells in medium being a hydrated state. Producing Raman maps based on the intensity of certain Raman bands attributed to be specific vibrational modes can also be a good way to locate the distribution of certain molecules within a cell. For example, a study used the 750 cm^{-1}, 1689 cm^{-1} and 2855 cm^{-1} Raman bands to map the distribution of mitochondria, protein and lipid molecules in live HeLa cell; [179]. Another study used confocal Raman microspectroscopy combined with immunofluorescence (IF) to record live single cell images. The aim of the study was to produce Raman based chemical maps which were similar to the IF images produced therefore, highlighting the potential for just using Raman spectroscopy for distinguishing healthy from infected or cancerous cells, without using traditional methods of staining and labelling. The study investigated single living LN-18 human glioma cells under cell culture conditions using both imaging techniques. Data was recorded using a water immersion objective (60x) equipped with a SHG Nd:YAG laser (532 nm, 22.5 mW). To ensure that contributing signal of the substrate holding the adhered cells was minimal and the Raman scattering from the cells was maximum, depth scans (x, z maps) were performed to determine the correct distance above the substrate for 2D imaging (x,y imaging); Depth results showed that roughly 2 µm was optimum. So as to compare with IF imaging, after a maximum of two image acquisitions per slide were recorded (~45-60 min per scan) the sample was washed with PBS, fixed in 4% phosphate buffered formalin solution for IF imaging. Raman spectra were then used to create chemical maps and identify different subcellular compartments (Cellular components such as the nucleus, Golgi apparatus, endoplasmic reticulum and mitochondria could be localised in Raman chemical images) equivalent to the multichannel IF images produced. Successful comparisons between the two techniques showed that Raman spectroscopy can produce meaningful images of cells equivalent to IF, but with the added advantage

that spectra from each colour classification of the cellular compartments can be extracted to explain biochemical differences between cellular structures. For detailed explanation on how Raman equivalent IF maps were created, see Klein [180].

A study in 2008 [21], aimed to produce spectral images of living cancer cells as a preliminary study to show the advantages of using Raman spectroscopy to produce non-destructive, label free chemical maps of living cells for characterisation of sub-cellular molecular structures for future disease diagnosis of single cells. However, firstly, they investigated which optical substrate would best preserve cell integrity for Raman measurement i.e. the most appropriate physiological conditions which won't seriously alter the cellular morphology or cell growth. The study used living Calu-1 cells (human lung cancer cells) as a cell model to test the different optical substrates (plastic, quartz, CaF_2 and ZnSe) using Raman microspectroscopy. Unfortunately the conventional culture substrate material, plastic (high Raman signal contaminating biological cell spectrum), is not appropriate for Raman measurements, therefore, using the BrdU assay and investigating the morphology of adhered cells through optical microscopy quartz, CaF_2 and ZnSe were evaluated for their ability to preserve cell integrity and growth conditions. BrdU assay, which evaluates the number of cells undergoing mitosis thus, cell growth, showed the quartz material to have a similar number of proliferating cells to plastic, with CaF_2 and ZnSe coming third and fourth respectively in the assay result. As ZnSe is toxic to cells the material produced an unsurprising 0% for the BrdU assay. Morphological investigation showed that cell morphology was conserved when using quartz and CaF_2, cells adopting the classical bipolar shape often observed with epithelial cancer cells. Raman spectra recorded from the nucleus of single living cells on either the quartz or CaF_2 substrate were comparable; therefore, both quartz and CaF_2 can be considered as equally adequate for Raman measurements. However, as quartz did not perturb cell growth it appeared to be the most appropriate material for the study of live cells in this model and was used in their study. For the study of the living cells, Raman signal were recorded from both the nucleus and the cytoplasm of 17 live cells seeded onto quartz. The spectral differences between the different cell regions were attributed to Raman signals associated with nucleic acid bases and the sugar-phosphate backbone. To get the true nucleus acid contribution though (nucleus is surrounded by cytoplasm), a spectrum recorded far from the nucleus (cytoplasm spectrum) was subtracted from a Raman signal recorded from a region inside the nucleus. The DNA residual was comparable with the calf thymus DNA reference signal, with some biochemical information from the proteins present in the nucleus (e.g. Phe at 1006 cm^{-1}). To elucidate the protein signal from the nucleus spectrum the DNA residual spectrum was subtracted from the nucleus spectrum and in a second step, the lipid contribution was

elucidated from the cytoplasm spectrum through subtracting the protein signal (cytoplasm will be a mix of lipids and protein contribution). The lipid cellular contribution in the cytoplasm spectrum showed good correlation to a reference spectrum. In addition, multivariate clustering algorithms were able to classify the spectra recorded from the different cell regions and K-means clustering was able to discriminate the nucleus and cytoplasm regions of the cell, as well as intracellular distribution maps of the nucleic acids, proteins, and lipids. This study therefore, demonstrates the feasibility of using Raman spectroscopy to prove cellular compartments of living cells, but also takes into consideration the effects of different optical substrates, and that a cell constitutes mixtures of macromolecular structures. The processing method described is a way of extracting the pure signals of certain macromolecules distributed in the cell structure.

A consideration of spontaneous Raman scattering is the low efficiency of the phenomenon. As a result, Raman spectral imaging requires extremely long acquisition times to produce a Raman spectral image of a single cell; to long for monitoring subtle molecular changes over time. Therefore a wealth of research has been dedicated to improving the low efficiency of the Raman signal for faster image acquisition speeds. One successful method is to measure Raman spectra at different points on the sample simultaneously instead of sequentially (the time it takes to record an image being decreased proportional to the number of detector points). For this method, many spectra can be acquired in a scan improving the speed of the Raman imaging. Palonpon *et al.* have demonstrated this through recording Raman images using a line shape focus, recording 400 Raman spectra simultaneously from the line illumination. Spectral image was constructed from 120 separate scanning lines with an exposure of 5 s per line, acquisition time for the full Raman was 16 min. When compared to the time it took Krafft and colleagues to construct a Raman image of a single cell (65 h accumulation time for a single image using Raman mapping) [181], this is major advance and allows the monitoring of certain cell functions, such as cell division, differentiation and apoptosis. The study by Palonpon clearly show the protein signals correlate with the chromosomes separating during cell division [179].

The combination of confocal microscopy and Raman imaging allows the user to collect Raman spectra of very small compartments and to collect high-resolution Raman images [182]. This powerful combination is proving valuable in the analysis of biological samples and living cells. A recent study by Scalfi-Happ *et al.* [182] showed the use of confocal Raman to image and resolve subcellular components of living neuroblastoma tumour cells based upon spectral information. Using a monolayer of neurblastoma cells on glass bottom Petri dishes, cluster analysis on the spectral region between 500 and 3100 cm^{-1} and spatial image information they were able to

separate cellular components of mitochondria or endoplasmic reticulum (based upon the vibrational band at 750, 1131, 1312 and 1585 cm^{-1} characteristic of cytochrome c), cytoplasma membrane (based upon lipids with major protein vibrations such as phenylalanine missing), cytoplasm (dominated by protein and lipid bands) and the nucleus (same bands as the cytoplasm but with higher 786, 1096 and 1344 cm^{-1} which can be assigned to adenosine). Combining this approach with that of Bonnier *et al.* [177] of growing the cells on matrigel or analysing a 3D spheroid culture would enable the high-resolution imaging of living cells in an environment that resembles the natural cellular microenvironment more closely. Seydou *et al.* [183] used 3D raman imaging to investigate the ability of lung cells to uptake asbestos in order to shine new light on the toxicity of asbestos. Based upon the Raman spectrum of the asbestos fibre and the cellular information they were able to provide 2D and 3D images highlighting the incorporation of short-length asbestos fibres into vesicles and the strength of high-resolution Raman imaging for toxicity studies. Furthering the use of confocal Raman imaging as a non-invasive tool capable of showing the distribution of cellular components a single endothelial cell was analysed to present the distribution of biochemical components using depth profiling and 3D projection [184]. With a 3D profile the authors were able to observe cell complexity with greater details using K means cluster analysis clearly discriminating seven classes of subcellular structure assigned to nucleolus, nucleoli, small organelles (e.g. mitochondria and endoplasmic reticulum), cytoplasm, cell membrane and cell membrane with adhesion proteins.

In order to provide a wider picture of the cellular changes occurring on single cells the combination of AFM and Raman has been investigated due to its ability to provide biophysical and biochemical information originating from the same cell. Lau *et al.* [185] have combined AFM imaging with confocal 3D Raman imaging. The study successfully showed the collection of Youngs modulus data and biochemical data on a brain tumour cell line (Figure 7). 3D confocal maps and AFM data correlate well in their ability to provide the volume of the cell and in addition 3D confocal Raman enables additional characterisation of organelles and lipid droplets and the volume estimation of organelles. Following on from the identification of subcellular domains exemplified by previous research in the area the estimation of organelle volume was enabled by the analysing and separating the voxel information contained with the Raman image based upon spectral localisation of organelles achieved using PCA. While the study highlights the value of the combined modalities in the potential monitoring of treatment efficacy and the effects of carcinogenic agents on cellular chemistry, architecture and biomechanics, the reality of such an approach routine cellular research

is hindered by the long time required to image each cell, rather this technique can be used to find biomarkers that are more easily identifiable by other techniques.

Surface Enhanced Raman Scattering (SERS)

SERS has also shown applicability for single cell detection. A study by Pallaoro *et al*. [186] demonstrated the use of SERS with biotags (SBTs) for the discrimination of cancerous and non-cancerous cells. Biotags were made from polymer-encapsulated silver nanoparticle dimers, which have been infused with unique Raman reporter molecules. The study showed that cancerous and non-cancerous epithelial prostate cells could be distinguished using a multiplexed ratiometric method, *in vitro*. Two sets of SBTs were used to target neuropilin-1 (NRP-1) receptors of cancer cells and the other targets both cancerous and no-cancerous cells through the HIV-derived TAT peptide (positive control (PC)). The NRP/PC ratioed signal, proved to be a robust quantitative measure of the overexpression of NRP-1 from cancerous cells. A further study by the group coupled SERS SBTs with a microfluidic device for investigating the use of the technique for in vivo classification of cancerous cells [187].

Recent developments in the use of SERS imaging has provided an excellent technique for specific multiplexed intracellular analysis. The authors point the reader to a tutorial review by Chourpa *et al.* [188]. Utilising nanoparticle SERS for intracellular imaging enables the specific analysis of cellular processes within live cells. Kneipp *et al.* have exemplified the use silver and gold nanoparticles, with an attached reporter molecule, as novel optical nanosensors for probing and imaging live cells [189]. Incubating mouse fibroblast cells with gold nanoparticles labelled with the well characterised Rose Bengal (RB) and Crystal violet (CV) reporter molecules they showed the ability of SERS imaging on live cells without photobleaching and the labels can be used over the entire visible and near infrared excitation wavelength range [190]. It was shown that the different labels localise to different areas within the cell with the RB nanoparticles localising to the cellular membrane and the CV nanoparticles localising in the centre of the cell. However, this differentiation is probably due to the properties of the label not any specific target molecules. Vo-Dinh and co-workers have shown the development of SERS based nanoprobes to enable single-cell sensing [191] using SERS nanoprobes functionalised with a reporter molecule (DNBA) and an antibody to epidermal growth factor showed the concentration across the cell. In addition Vo-Dinh has provided a nanosensor that is capable of monitoring the apoptosis in living cells by measuring caspase activity, probing an important intracellular marker in a reproducible and specific manner. The use of SERS imaging is not limited to just intracellular analysis. Hodges *et al.* have combined immunolabelling and SERS in the study of cell

membranes [192]. Hodges and co-workers applied gold conjugated antibodies coupled with sliver enhancement to attached silver nanoparticles to the cell surface enabling direct information on the cell membrane without the use of reporter molecules. The future use of this technique when combined with imaging will provide detailed information on structural changes that occur within cellular membranes over many cellular processes.

Tip Enhanced Raman Spectroscopy (TERS)

Tip Enhanced Raman spectroscopy (TERS) is a nano-spectroscopic technique that uses the surface enhancement phenomenon associated to a metal tip, similar to the ones used with Atomic Force Microscopy [241-243], a thin coating of Ag or Au in the AFM tip dramatically boost the Raman signal via excitation of surface Plasmon plartions in a diameter of approx. 10 nm around the tip. Böhme *et al*. investigated supported lipid structures and human cells using tip-enhanced Raman spectroscopy (TERS) to correlate the results obtained from lipid layers with TERS experiments on human cells [193]. TERS is a label-free and fast technique and unlike other alternative methods of visualising cellular actions, there is no requirement for different labels to be used which themselves may influence cellular activity. The study by Böhme and co-workers suggests that TERS measurements obtained within the study show the potential of the technique as a fast detection tool when determining structural changes on a nano-metre scale. One disadvantage of TERS is that spectra collected from the same area in both lipid surface and cell surface measurements exhibits different features. One of 3 spectra measured on the lipid surface contained symmetric and asymmetric O-P-O stretching at 758 cm^{-1} and 822 cm^{-1}, respectively. Stretching from C=O occurring at 1725 cm^{-1} is feature characteristic of the lipid head group. The 2 remaining spectra from the lipid layer exhibit various vibrations from symmetric PO_2 stretching at 1080 cm^{-1} and C=O at 1753 cm^{-1} to the modes characteristic of aliphatic residue. The presence of a lipid structure can be determined by the characteristic Raman modes of the phosphate containing head groups. In comparison to the TERS spectra collected from a lipid layer, TERS spectra collected on a human epidermal derived keratinocyte contained strong lipid contributions and vibrations of O-P-O (symmetric and asymmetric) at 780 cm^{-1} and 810 cm^{-1}, plus PO_2 stretching modes occurring at 1095 cm^{-1} (symmetric) and at 1219 cm^{-1} (asymmetric).

TERS has the potential to be used as a tool to investigate the surface of a cell and to assess cell-drug interactions, possibly *in vivo*, with short sampling times. However, cautions must be taken when using TERS due to the contamination risk the tip faces when coming into contact with a sample or substrate as this can cause incorrect spectral assignments to be assigned and conclusions to be

drawn from the results. Budich *et al.* studied a control experiment where the TERS tip is allowed to be contaminated by surface contact. Contamination occurs when the tip comes into contact with cell wall components and other material from the substrate. Budich *et al.* reported that the easiest way to overcome contamination issues is to clean the tip and check that it is clean by detecting a TERS signal from a clean substrate [194]. TERS has the ability to distinguish membrane components, DNA and amino acids with nano-metre resolution, thus it has the potential to be an invaluable tool which can be employed to understand currently unknown cellular mechanisms, actions and drug interactions.

Raman Tweezers

Raman tweezers combines Raman spectroscopy with optical trapping. The technique of optical trapping was pioneered by Arthur Ashkin in 1970 [14, 195-196]. Optical trapping is used to trap cells through the use of a highly focused laser beam. Once a cell is trapped and isolated, a Raman measurement from the trapped cell can then be acquired. It has the added advantage of no intercellular and surface adhesion effects at the cellular level. For more details on this technique please refer to Snook *et al*. [14, 196] This setup allows the trapping and spectroscopic interrogation of live cells being traversed through a microfluidic device, and has applications for cellular screening. An early study using Raman tweezers, showed the potential of the technique through analysing 200 normal and 200 cancerous colorectal cells using PC fed ANNs to classify the cell spectra recorded. The analysis result produced a score of 86.3% for both sensitivities and specificities [182, 196]. Other earlier studies using Raman tweezers for both fixed and live cell classifications, include a study on single live red and white blood cells under physiological conditions [197], the identification of leukaemia cells using both PCA and PCA-LDA (on average, 95% and 90% of patient cells were accurately classified into their respective cell types. Cancer cells exhibiting a lower DNA to protein ratio than normal cells, attributed to the increased metabolic rate of the cancers cells) [198], the classification of chemical fixed urological cells (the goal being to develop a high-throughput diagnostic method for the detection of prostate cancer cells present in urine after they have been shed into urine by the prostate. Sensitivities and specificities of >93% and 98% respectively were achieved for formalin fixed cells) [199], erythrocytes, leukocytes, acute myeloid leukaemia cells (OCI-AML3) and breast tumour cells (BT-20 and MCF-7) [200], human herpesvirus-8 (HHV-8) infected hematopoietic cells (tumour causing virus) and uninfected (infected cells showed an increase in intensity from the 1004, 1093 and 1664 cm^{-1} bands, with respect to uninfected hematopoietic cells) [201] and the spectroscopic effect of alcohol on single red blood cells using a near infrared laser;

spectral analysis results showing the intensity of the Raman band at 752 cm-1 to decrease after the administration of alcohol [202].

Raman Activated Cell Sorting (RACS)

Raman activated cell sorting (RACS) would allow for the analysis of cells without the use of exogenous labels, which are disruptive of cellular chemistry. With the potential of Raman tweezer setups being evident, a study by Lau *et al*. [203] proposes the use of Raman tweezers with novel multichannel microfluidics to create an optofluidic RACS device. The basic idea of a RACS system is not unlike the design of a conventional flow cytometry instrument, focusing a stream of cells towards a laser beam for spectral analysis, which is then followed by sorting cells' based on the spectral fingerprint recorded. However, the acquisition time to record a Raman signal from a single cell is long. This means that while the cell is trapped, other cells flowing downstream may knock the trapped cell out of the laser focus or also get trapped by the laser thus, interfering the spectral signal being recorded. Therefore, new microfluidic device designs are needed for a RACS system. In this study, two different optofluidic designs were evaluated for their sorting design and flow velocity effect for identifying and sorting two different leukaemia cell lines (i) hydrodynamic focusing and (ii) pinch-flow fractionation. Both designs consist of multiple channels, one is designed as inlet channel for the delivery of the cells in solution into the device, while channels adjacent to the inlet channel are used as sorting channels. Laser trap is placed in the center of the inlet channel, and once a flowing cell is trapped, the laser pulls it to a side of the inlet for Raman signal acquisition. Once classified, the cell can then be released into correct sorting channel associated with the classification. Cells not trapped are recycled and looped back into the inlet channel. The hydrodynamic focusing design is a similar concept to that it which is used in commercial FACS instruments. However, the study showed that high efficiency trapping of lymphocyte cells (diameter of μm) required a particle flow velocity of less than 400 μm^{s-1}. The hydrodynamic focusing design suffered from pressure fluctuations though when low velocities (<400 μm^{s-1}) were used, therefore, this design was more suited for higher flow velocities coupled with higher powered trapping lasers that can offer greater trapping stability (For more information on the design of the two microfluidic devices [203]. As a result, the pinch-flow fractionation design was evaluated with pre-B lymphoblast B cell lymphoma and a T lymphomblast (acute lymphoblastic leukemia) cells. Cells were suspended in DPBS (Gibco) and 20 of each cell type were samples with the Raman tweezers, acquisition time of 120 s for each spectrum. The cell spectra recorded were then analysed using PCA, which was able to group the spectra from the two cell types. The spectral data obtained could then be used as the

training set in a Chemometric model to identify unknowns flowed through the RACS device. Experimental results also showed that cells exposed to a 660 nm laser were still viable. In this study, a Raman based RACS system has been demonstrated as a proof of concept, combining Raman tweezers coupled with a microfluidic device to successfully identify cells based on the Raman spectral signatures recorded and highlights the potential of the setup for sorting capabilities; in a low throughput manner [203-204]. A further study [200], by the Popp group, investigated the use of two different optical traps for a RACS device. The first design was based on a quartz capillary coupled to a Raman microscope, with a 786 nm excitation laser. The second used a microfluidic chip that accommodated laser fibres of the optical trap. This second design had capabilities to separate cells and sort them based on their Raman based classification. The multifunctional microfluidic chip was made of glass employing a 514 nm excitation laser so as to reduce low background signals of glass. For the Raman chip, cells' were traversed through the centre of the chip using hydrodynamic focusing as it was more advantageous trapping cells in the in the middle of the microfluidic channel. Cells' could then be sorted into sorting channels after spectroscopic measurement through flow switching. The study showed a much improved Raman acquisition time than Lau *et al.* 10 s being needed per cell, compared to 120 per cell. LDA classification models were able to distinguish the Raman cell spectra recorded, with design one producing classification accuracies of 95%, 97.2%, 94.5% and 94.6% for erythrocytes, leukocytes, BT-20, OCI-AML3 cells' respectively (LDA model scores were evaluated using 10-fold cross validation). Lower accuracies of 60% were obtained for MCF-7 cells (15 out of 25). However, most of the misclassified MCF-7 were assigned to the other breast carcinoma cell line, BT-20 (8 out of 10 misclassified). For the second design, classification accuracies of 96.3%, 95.4%, 86.2% and 96.2% were achieved for OCI-AML3, MCF-7, leukocytes and BT-20 cells respectively. For the second design the optical trap was unable to trap showed erythrocytes, suggested to be due to their smaller diameter, however, the spectra produced were of better quality. Classification results were comparable with previous studies on dried and fixed cells. This study, again, highlights the potential of Raman spectroscopy for RACS. If the classification was synchronised with the microflow control, RACS would become possible with the microchip design demonstrated. However, to get to a point of fully automated cell sorting will require data processing (baseline correction, background subtraction, laser line correction and classification according to a model build with a training dataset) in real time, which may be a little while off. A further study by the same group used an improved method for background correction and also improved the microchip design by making the chip out of quartz (quartz has a much reduced background signal than glass in the fingerprint spectral region when using a near-infrared laser excitation) [205].

Proposed RACS devices, however, all have a problem with reduced throughput because of the high acquisition times needed. This is not practical for single cell sorting and a direct result of the weak Raman signal, thus, low S/N and many co-averaged scans are needed to produce a good single cell spectrum. For Raman spectroscopy, only 1 in 10^{6-8} photons undergoes spontaneous Raman scattering [204]. In order to overcome this attempts have been made to increase the Raman signal using resonance Raman scattering (RRS), coherent anti-stokes Raman scattering (CARS), stimulated Raman scattering (SRS) and surface enhanced Raman scattering (SERS) [204]. A study in 2009 investigated the use of multiplex CARS (MCARS) for cell sorting. MCARS excites multiple transitions simultaneously, producing a broadband spectrum with similar wealth to a traditionally recorded Raman spectrum, but with the advantage of much greater signal intensities, ideal for high throughput cell sorting and high speed cell detection. Camp *et al*. coupled MCARS with a microfluidics to determine different polymer beads of the same size but different compositions. The demonstrated clear distinction between the different beads in aqueous solution, therefore, showing the potential for MCARS coupled with microfluidics to sort single cells, in a methodology similar to FACS. MCARS could provide additional information to flow cytometry, possible replacing fluorescent labels [206]. However, the Notingher group took a different tact when trying to improve the Raman acquisition time. The study achieved acquisition times of ~5 s per cell through focusing a laser beam to a line instead of raster scanning a cell. Prediction accuracies of >95% specificity and sensitivity were achieved even with though test spectra contained a relatively high level of noise (test spectra were recorded using a 5 s acquisition, while training set were recorded over 10 minutes). Authors also state that focusing the laser beam in a line across the cell and focusing the Raman scattered photons on the entrance-slit of the spectrometer would speed up acquisition times with no raster scanning needed. It also stated that the use of high powered lasers could also speed up acquisition times in the futures potentially enabling sorting speeds of 8 cells per s [207]. This development in speed and portability is required in order to provide rapid sorting of cells based upon direct spectral information and will be of interest in a personalised medicine future where analysis of personalised patient samples may be required.

Coherent Anti-Stokes Raman Spectroscopy (CARS) and Stimulated Raman Scattering (SRS)

CARS and SRS are exciting techniques that offer the user the potential of real-time label-free imaging of live cells based upon molecular information obtained directly from the biochemical constituents of the cell under analysis. In particular CARS has excellent potential as a live cell lipid imaging technique. In the CH_2 stretching vibrations of the Raman spectrum a strong band appears at 2845

cm^{-1} attributed to the symmetric stretching of CH_2 groups [69]. A strong CARS signal at this frequency enables CARS to be very sensitive to changes in lipid composition with the highest contrast coming from lipid droplets [69]. CARS images collected at 2845 cm^{-1} have analysed the live conversion of 3T3-LI fibroblast cells to fat cells [70]. Whilst fluorescence microscopy can monitor the dynamic of cellular processes over similar time frames as CARS the observation of long range cellular processes by fluorescence it is not suitable because of cellular degradation of the dyes [70]. In addition to observing the long term differentiation of fibroblast to cell lines (from 0h to 192h) Nan *et al*. were able to observe the effect of different sample preparation techniques on the lipid droplets within the fibroblast cells and concluded that Oil Red O (a fluorescent dye) staining of fixed cells caused aggregation of lipid droplets whereas formaldehyde fixation and Nile red staining had no effect on the lipid droplets. Proving CARS as a powerful technique for direct, live cell information with chemical selectivity. However it should be noted that it is not possible to distinguish which lipids are responsible for any process / localisation based upon the CARS spectrum, in order to determine this isotopic labelling studies (with deuterium) are required. Deuterium isotopic labelling was able to show the differential uptake of eicosapentaenoic acid (EPA) and deuterated oleic acid by rat hepatocyte cells as the CD bond stretching frequency is observed in a relatively silent region of the biological Raman spectrum near 2100 cm^{-1} [71]. Interestingly this studies showed colocalisation of both acids in lysosomes where incubation of cells with either single acid resulted in sequestration in small Lipid droplets for oleic acid and into lysosomes for EPA, indicating that fatty acids such as EPA change the way cells process normal fatty acids [71]. A interesting use of CARS coming with plasmon resonance enhanced four wave mixing (FWM) was demonstrated by the Moger Group [208]. Garrett *et al.* used this technique to visualize the distribution of gold nanoshells in live cells combining the plasmon enhanced FWM image with CH_2 CARS signal to show the position of the nanoshells within living cells, showing that clusters of nanoshells are visible throughout the cytoplasm. In addition this study examined the impact of H_2S on the cellular uptake of nanoshells showing a rapidly releasing donor of H_2S resulted in high uptake levels. SRS enables the rapid imaging of components like CARS but does not suffer from the nonresonant background and spectral distortion. SRS has been shown highly valuable in the label-free live-cell imaging of nucleic acids [63]. Imaging of nucleic acids is important for the investigation of many cellular processes, the ability to collect this label-free so as to not interrupt any cellular processes is of extreme interest. Zhang *et al.* imaged the distribution of nucleic acids at 785 cm^{-1} (symmetric phosphodiester stretch, ring breathing modes of pyrimidine bases), Amide I at 1655 cm^{-1}) and a lipid specific image at 2845 cm^{-1}. Clearly highlighting the chromosomes in a combined image and showing the ability of SRS to image in the fingerprint region of the Raman spectrum whereas CARS is mainly used for the CH_2 stretching

region. In addition, this study has shown the ability of SRS imaging to determine the cell cycle phase based upon variations in the signal from nucleic acid SRS response [209]. SRS was able to provide information on which cells are undergoing / preparing for division and which are not an important function to be able to analyse on live cells to further research the myriad of problems caused for overactive / underactive cellular duplication.

Future of Vibrational Spectroscopy for Cytology and Cellular Research

This review has highlighted major trends and drivers within cellular spectroscopy and in order to look towards the future the following areas will need to be taken into account.

A number of studies have favoured recording average cell spectra rather than recording spectral information from single cells. Although averaging spectra can improve classification accuracies, an average cell spectrum of a population of cells effectively removes information regarding molecular variations at the single cell level [105]. For cellular diagnosis, it is important to understand the spectral profile of normal molecular changes as well as disease at the single cell level. Also, when studying the molecular effects of external agents it is important to understand the spectral profile of cell cycle phases as well as cell death. Therefore, the study of single cells should be paramount.

The introduction of FPA detectors to standard benchtop IR instruments and developments in Raman microscopy has made single cell studies easily accessible. The combination of vibrational spectroscopy with micro-devices has also shown that cells can be investigated *in situ*. An advantage of this setup is the increased DNA information from hydrated/live cells. Due to DNA transcribing all of the genetic instructions used for the functioning of a living cell, changes to nucleic acid molecular structures may well be early spectral biomarkers of disease. Therefore, investigating cells in a hydrated/live environment may be a more likely way to find such spectral biomarkers. However, although micro devices have been successfully in overcoming the water barrier, for FTIR, their design and fabrication often require specialist resources, especially microfluidic devices. Static micro compression devices are commercially available but they suffer from short operation times due to the medium leaking outside of the chamber [147-149]. Technological developments have also enabled acquisition of spectra with high S/N that is required to probe sub cellular compartments and single cells.

One area of instrumentation that needs to be developed for the future of imaging within cytological processes is the time for collection. Minutes are to slow if IR spectroscopy is to be ever used to identify and sort cells based on the biochemical signal recorded. Quantum cascade lasers are under rapid development and can produce a high brightness that will take the sensitivity of FTIR-MS to the

next level [210].One demonstration of lasers being used to investigate single cells is a study by Amrania *et al.* [210] in the study a laser based table top IR spectroscopic micro-imaging system was used to obtain vibrational fingerprint signatures of living human ovarian cancer cells. The bright laser pulses resulting in spectral images with high S/N being produced with ~100 psec image acquisition times, roughly 1011 times faster than current mid-IR imaging techniques. This has shown that certain laser sources can dramatically exceed current FTIR capabilities, potentially revolutionising the field of IR spectroscopy for cellular discrimination and diagnosis. In Raman, the use of single cell spectroscopy has been shown to be possible of discriminating spectra form five oral bacteria with a short collection time [75] enabling the rapid discrimination and possible forward use via RACE in personalised medicine of the future. CARS and SRS have shown great promise and offer great opportunities for rapid real time imaging of single cells for a multitude of applications.

As ever, data considerations are of great importance. Further analysis is required on the reproducibility and effect of sample preparation on vibrational spectra and there is a need for large scale trials of these technologies in order to discover this content. Fundamentals of data processing, in particular for Raman, need to be further understood in order to enable a coherent approach and spectral marker discovery for the accurate investigations and discrimination of cells from different sources. In order for the processing to equal the advances in technology there is a requirement to provide real time processing which will mean a move away from the standard approaches of dimensionality reduction and place a greater emphasis on spectral feature extraction and learning. In addition, with a greater movement to portability and mobility there is a need to unleash data from the desktop. A recent study has shown the ability to perform spectral manipulation and pre-processing on mobile devices, releasing the analytical scientist form the bench [211].

The future of vibrational spectroscopy for cytological research is brilliant and bright. Raman spectroscopy holds amazing potential for label free direct imaging of single cells in real time and, in the future, could replace such well characterised methodologies such as FACS and fluorescence microscopy. FTIR is undergoing technological developments shifting the focus from Globars to QCLs provides opportunities to speed up spectral acquisition with possible increase in S/N for single cell studies. Overall, there is a need to introduce large scale trials to correctly assess all the components (sample preparation, spectral collection and spectral analysis) required in a spectroscopic study for the benefit of the cytological and cellular research domain.

Acknowledgements

MJB would like to thank *Analyst* for their kind invitation to write this article. MJB, JRH and GC are grateful to EPSRC, Dstl, Rosemere Cancer Foundation, Fera, Sydney Driscoll Foundation, Brain Tumour North West, Association for British Spectroscopists, The Royal Society and the NIHR for their support for their support. KMD thanks Agilent for their support.

References

[1] Dictionary.com (http://dictionary.reference.com/browse/cell) Accessed on 3rd February 2014

[2] Hooke, R., *Micrographia*, Royal Society Library Archives, 1665

[3] Royal Society Website (http://royalsociety.org/events/2014/micrographia/) Accessed on 3rd February 2014

[4] Baluska, F., Volkmann, D., Barlow , P.W., *Ann. Bot.*, 2004, **94**, 9-32

[5] Cao, J., Ng, E. S., McNaughton, D., Stanley, E. G., Elefanty, A., Tobin, M. J., Heraud, P., *Int. J. Mol. Sci*, 2013, **14**, 17453-17476

[6] Downes A., Mouras, R., Elfick, A., *J. Biomed. Biotechnol.*, 2010, doi: 10.1155/2010/101864

[7] Keller, M.D., Kanter, E.M., Mahadevan-Jansen, A., *Spectroscopy,* 2006, **21**, 33-39

[8] Thompson, T., *Laser Focus World*, Editorial Digest

[9] Mahadevan-Jansen, A., *Biomedical Photonics Handbook*, ed. Vo-Dinh, T., CRC Press, Washington DC, 2003, 20:1, pp.30:27

[10] Taleb, I., Thiefin, H., Gobinet, C., Untereiner, V., Bernard-Chabert, B., Heurge , A, Truntzer , C., Hillon, P., Manfait, M., Ducoroy, P., Sockalingum, G.D., *Analyst*, 2013, **138**, 4006-4014

[11] Fullwood, L.M., Clemens, G., Griffiths, D., Ashton, K., Dawson, T.P., Lea, R.W., Davis, C., Bonnier, F., Byrne, H.J., Baker, M.J., *Anal. Methods*, 2014, **6**, 3948-3961

[12] Jarvis, R.M., Goodacre, R., *FEMS Microbiol. Lett.*, 2006, **232**, 127-132

[13] Ellis, D.I, Cowcher, D.P., Ashton, L., O'Hagan, S., Goodacre, R., *Analyst*, 2013, **138**, 3871-3884

[14] Faria, E. C., Gardner, P., *Single Cell Analysis Methods and Protocols Methods Mol. Biol.*, 2012, **853,** Part 12

[15] Byrne, H., Sockalingum, G., Stone, N., *Biomedical Applications of Synchrotron Infrared Microspectroscopy*, Royal Society of Chemistry, RSC Analytical Spectroscopy Monographs, 2011, **11**, 105-142

[16] Huang, W. E., Mengqui, L., Jarvis, R. M., Goodacre, R., *Adv. Appl. Microbiol.*, 2010, **70**, 153-186

[17] Chan, J. W., Lieu, D. K., *J. Biophotonics*, 2009, **2**, 656-686

[18] Baker, M.J., Gazi. E., Brown, M.D., J.H. Shanks, Gardner, P., Clarke, N.W., *Brit. J. Cancer.*, 2008, 99, 1859-1866

[19] Baker, M.J., Clarke, C., Demoulin, D., Nicholson, J.M., Lyng, F.M., Byrne, H.J., Hart, C.A., Brown, M.D., Clarke, N.W., Gardner, P., *Analyst*, 2010, **135**, 887-894

[20] Goodacre, R., Timmins, E.M., Burton, R., Kaderbhai, N., Woodward, A.M., Kell, D.B., Rooney, P.J., *Microbiol.,* 1998, **144**, 1157-1170

[21] Draux, F., Jeannesson, P., Beljiebbar, A., Tfayli, A., Fourre, N., Mafait, M., Sule-suso, J., Sockalingum, G. D., *Analyst*, 2009, **134**, 542-548

[22] Bassan, P., Kohler, A., Martens, H., Lee, J., Byrne, H.J., Dumas, P., Gazi, E., Brown, M., Clarke, N., Gardner, P., *Analyst*, **135**, 2010, 268-277

[23] Bassan, P., Kohler, A., Martens, H., Lee, J., Jackson, E., Lockyer, N., Brown, M., Clarke, N., Gardner, P., *Journal of Biophotonics*, **3**, 2010, 609-620

[24] van Dijk, T., Mayerich, D., Carney, S., Bhargava, R., *App Spectrosc.*, 2013, **67**, 546-552

[25] Filik, J., Frogley, M.D., Pijanka, J.K., Wehbe, K., Cinque, C., *Analyst*, 2012, **137**, 853-861

[26] Cao, J., Ng, E. S., McNaughton, D., Stanley, E.G., Elefanty, A.G., Tobin, M.J., Heraud, P., *Analyst*, 2013, **138**, 4147-4160

[27] Banwell, C.N., McCash, E.M., *Fundamentals of Molecular Spectroscopy*, Fourth Edition, McGraw-Hill, London, 1994

[28] Hopkins, R., Pelfrey, S.H., Shand, N.C, *Analyst*, 2012, **137**, 4408-4410

[29] Bonnier, F., Ali, S.M., Knief, P., Lambkin, H., Flynn, K., McDonagh, V., Healy, C., Lee, T.C, Lyng, F.M, Byrne, H.J, *Vibrational Spectroscopy*, 2012, **61**, 124-132

[30] Lombardi, J. R., Birke, R. L., *J. Chem. Phys.*, 2012, **136**, 144704-1 **–** 144704-11.

[31] Lyng, F.M, Gazi, E., Gardner, P., *Preparation of Tissues and Cells for Infrared and Raman Spectroscopy and Imaging in Biomedical Applications of Synchrotron Infrared Microspectroscopy (Moss D. ed.)*, RSC Analytical Spectroscopy Monographs No. 11, Royal Society of Chemistry, 2011, 147-185

[32] Gazi, E., Gardner P., Lockyer, N.P., Hart, C.A., Clarke, N.W., Brown, M.D., *J. Lipid Res.*, 2007, **48**, 1846-1856

[33] Meade, A.D., Clarke, C., Draux, F., Sockalingum, G.D., Manfait, M., Lyng, F.M, Byrne, H.J, *Anal. Bioanal. Chem.,* 2010, **396,** 1781 – 1791

[34] Mariani, M.M., Lampen, P., Popp, J., Wood, B.R., Deckert, V., *Analyst*, 2009, **134**, 1154-1161

[35] Trevisan, J., Angelov, P.P., Carmichael, P.L, Scott, A.D., Martin F.L., *Analyst*, 2012, **137**, 3202-3215

[36] National Science Foundation Microbe Factsheet http://www.nsf.gov/bio/mcb/microbe/factsheet.pdf. Accessed on 5th March 2014

[37] Bretzel, W., Schurter, W., Ludwig, B., Kupfer, E., Doswald, S., Pfister, M., van Loon APGM, *Journal of Industrial Microbiology & Biotechnology,* 1999, **22**, 19-26

[38] Helm, D., Labischinski, H., Schallehn, G., Naumann, D., *Microbiology*, 1991, **137**, 69-79

[39] Naumann, D., Helm, D., Labischinski, H., *Nature*, 1992, **351**, 81-82

[40] Puppels, G.J., De Mul, F.F.M, Otto, C., Greve, J., Robert-Nicoud, M., Arndt-Jovin, D.J., Jovin, T.M., *Nature*, 1990, **347**, 301-303

[41] Goodacre, R., Timmins, E.M., Burtin, R., Kaderbhai, N., Woodward, A.M., Kell, D.B., Rooney, P.J., *Microbiology*, 1998, **144**, 1157-1170

[42] Maquelin, K., Kirschner, C., Choo-Smith, L.P., van den Braak, N., Endtz, H.Ph., Naumann, D., Puppels, G.J., *Journal of Microbiological Methods*, 2002, **51**, 255-271

[43] Beekes, M., Lasch, P., Naumann, D., *Vet. Microbiol*, 2007, 123, 305-319

[44] Harz, M., Rösch, P., Peschke, K.-D., Ronneberger, O., Burkhardt, H., Popp, J., *Analyst*, 2005, **130,** 1543-1550

[45] Barrington, S.J., Bird, H., Hurst, D., McIntosh A.J.S, Spencer, P., Pelfrey, S.H., Baker, M.J., *Proc. SPIE 8358, Chemical, Biological, Radiological, Nuclear, and Explosives (CBRNE) Sensing XIII*, 2012, 83580E doi:10.1117/12.915707

[46] de Siqueira e Oliveria, F.S., Giana, H.E., Silveira, L. Jr., *J. Biomed. Opt.*, 2012, **17**, doi: 10.1117/1.JBO.17.10.107004

[47] Meisel, S., Stöckel, S., Elschner, M., Melzer, F., Rösch, P., Popp, J., *Applied and Environmental Microbiology*, 2012, **78,** 5575-5583

[48] Nicolaou, N., Goodacre, R., *The Analyst*, 2008, **133**, 1424-1431

[49] Ellis, D.I., Broadhurst, D., Kell D.B., Rowland, J.J., Goodacre, R., *Applied and Environmental Microbiology*, 2002, **68**, 2822-2828

[50] Brandily, M.L., Monbet, V., Bureau, B., Boussard-Pledel C., Loreal O., Adam, J.L., Sire, O., *Sensors and Actuatirs B: Chemical,* 2011, **160**, 202-206

[51] Argyri, A.A., Jarvis, R.M., Wedge,D., Xu, Y., Panagou, E.Z., Goodacre, R., Nychas, G.J.E, *Food Control*, 2013, **29**, 461 – 470

[52] Davis, R., Deering, A., Burgula, Y. Mauer, L.J., Reuhs B.L., *Journal of Applied Microbiology*, 2011, **112**, 743-751

[53] Dire, D. J., "CBRNE – Biological Warfare Agents", http://emedicine.medscape.com/article/829613-overview. Accessed on 01 April 2014

[54] Manchee, R., Broster, M., Melling, J., Henstridge, R., *Nature*, 1981, **294**, 254-255

[55] Samuels AC, Snyder AP, St. Amant D, Emge DK, Minter J, Campbell M, Tripathi A (2008).

CBRNE Sensing Proc. of SPIE, p.695413

[56] McIntosh, A.J.S, Barrington, S.J., Bird, H., Hurst, D., Spencer, P., Pelfrey, S., Baker, M.J., *Anal. Bioanal Chem.*, 2012, **404**, 2307-2315

[57] Jarvis, R.M., Brooker, A., Goodacre, R., *Faraday Discussions*, 2006, **132**, 281-292

[58] Hermelink, A., Brauer A., Lasch P., Naumann D., *Analyst*, 2009, **134**, 1149-1153

[59] Zhang, X., Young M.A., Lyandres, O., Van Duyne, R.P., *JACS*, 2005, **127**, 4484 - 4489

[60] Sengupta, A., Shende, C., Farquharson S., Inscore, F., *International Journal of Spectroscopy,* 2012, **2012**, Article ID 176851

[61] Faulds, K., Barbagallo, R.P., Keer, J.T., Smith, W.E., Graham, D., *Analyst*, 2004, **129**, 567-568

[62] Gracie, K., Correa, E., Mabbott, S., Dougan, J.A., Graham, D., Goodacre, R., Faulds, K., *Chemical Science*, 2014, **5**, 1030 – 1040

[63] Schuster, K.C., Reese, I., Urlaub, E., Gapes, J.R., Lendl, B. *Anal. Chem.* 2000, **72,** 5529-5534

[64] Xie, C., Mace, J., Dinno, M.A., Li, Y.Q., Tang,W., Newton R.J., Gemperline, *Anal. Chem,* 2005, **77**, 4390 - 4397

[65] Chan, J.W., Esposito, A.P., Talley, C.E., Hollars, C.W., Lanes, S.M., Huser, T., *Anal. Chem.* 2004, **76**, 599-603

[66] Zhou, A.H., McEwen, G.D., Wu, Y.Z., Combined AFM/Raman microspectroscopy for characterisation of living cells in near physiological conditions in *Microscopy: Science, Technology, Applications and Education, A Mendez-Vilas and J Diaz Eds*, 2010, 515 – 522

[67] Pätzold, R., Keuntje, M., von Ahlften, A.A., *Anal. Bioanal. Chem,* 2006, **386**, 286-292

[68] Cheng, J., Xie, X. S., *J. Phys. Chem.*, 2004, **108**, 827-840

[69] Nan, X., Yaung, W.Y., Xie, X.S., *Biophotonics International,* 2004**, 11**, 44-47

[70] Nan, X., Cheng, J.X., Xie, X.S., *J. Lipid. Res.*, 2003, **44**, 2202-2208

[71] Evans, C.L., Xie, X.S., *Annu. Rev. Anal. Chem.*, 2008, **1**, 883-909

[72] Pestov, D., Wang, X., Ariunbold, G.O., Murawski, R.K., Sautenkov, V.A., Dogairu A., Sokolov, A.V., Scully, M.O., *PNAS*, **15**, 422-427

[73] Petrov, G.I., Arora, R., Yakovlev, V.V., Wang, X., Sokolov, A.V., Scully, M.O., *PNAS*, 2007, **104**, 7776-7779

[74] Scully, M.O., Kattawar, G.W., Lucht, R.P., Opatrny, T., Pilloff, H., Rebane, A., Sokolov, A.V., Zubairy, M.S., *PNAS*, 2002, **99**, 10994-11001

[75] Wang, Y., Ji, Y., Wharfe, E. S., Meadows, R. S., March, P., Goodacre, R., Xu, J., Huang, W. E., *Anal. Chem*, **85**, 10697-10701

[76] Chow, A. Y. , Cell Cycle Control by Oncogenes and Tumor Suppressors: Driving the Transformation of Normal Cells into Cancerous Cells. *Nature Education,* 2010, **3(9)**, 7-9

[77] Knowles, M., Selby, P., in *Introduction to the Cellular and Molecular Biology of Cancer,* 4th ed. Oxford University Press, Oxford, 2005

[78] Cancer Research UK (www.cancerresearchuk.org). Accessed on 27th March 2014

[79] Wood, B. R., Kiupel, M., McNaughton, D., *Vet. Pathol.*, 2013, **51**, 224-237

[80] Bassan, P., Kohler, A., Martens, H., Lee, J., Byrne, H. J., Dumas, P., Gazi, E., Brown, M., Clarke, N., Gardner, P., *Analyst*, 2010, **135**, 268-277

[81] Jamin, N., Dumas, P., Moncuits, J., Fridman, W. H., Teillaud, J. L., Carr, G. L., Williams, G. P., *Proc. Natl. Acad. Sci. USA.*, 1998, **95**, 4837-4840

[82] Miller, L. M., Smith, G. D., Carr, G. L., *J. Biol. Phys.*, 2003, **29**, 219-230

[83] Holman, H. N., Martin, M. C., Blakely, E. A., Bjornstad, K., McKinny, W. R., *Biopolymers (Biospectroscopy)*, 2000, **57**, 329-335

[84] Holman, H. N., Martin, M. C., McKinny, W. R., *Spectroscopy*, 2003, **17**, 139-459

[85] Holman, H. N., Goth-Goldstein, R., Martin, M. C., Russell, M. L., McKinney, W. R., *Environ. Sci. Technol.*, 2000, **34**, 2513-2517

[86] Wood, B. R., Quinn, M. A., Tait, B., Ashdown, M., Hislop, T., Romeo, M., McNaughton, D., *Biospectroscopy*, 1998, **4**, 75-91

[87] Romeo, M., Burden, F., Quinn, M., Wood, B., McNaughton, D., *Cell. Mol. Biol.*, 1998, **44**, 179-187

[88] Romeo, M., Quinn M., Wood, B. R., McNaughton, D., in *Spectroscopy of Biological Molecules: New Direction*, SpringerLink, Oxford

[89] Diem, M., Romeo, M., Miljkovic, M., Matthaus, C., *Analyst*, 2004, **129**, 880-885

[90] Lasch, P., Pacifico, A., Diem, M. *Biopolymers*, 2002, **67,** 335–338

[91] Lasch, P., Boese, M., Pacifico, A., Diem, M., *Vibrational Spectroscopy*, 2002, **28**,147-157

[92] Lasch, P., Chiriboga, L., Yee, H. Diem, M., *Technol. Cancer Res. Treat.*, 2002, **1**, 1-5

[93] Diem, M., Romeo, M., Matthäus, C., Miljkovic, M., Miller, L.M., Lasch, P., *IR Phys. Technol*, 2003, **45**, 31–118

[94] Pacifico, A., Chiriboga, L. A,, Lasch, P., Diem, M., *Vibrational Spectroscopy*, 2003, **32**, 107-115

[95] Diem, M., Romeo, M., Matthäus, C., Miljkovic, M., Miller, L. M., Lasch, P., *IR Phys. Technol*, 2003, **45**, 31–118

[96] Diem, M., Chiriboga, L., Lasch, P., Pacifico, A., *Biopolymers*, 2002, **67**, 349-352

[97] Diem, M., Boydston-White, S., Chiroboga, L., *Applied Spectroscopy*, 1999, **53**, 144-171

[98] Boydston-White, S., Gopen, T., Houser, S., Bargonetti, J., Diem, M., *Biospectroscopy*, 1999, **5**, 219-227

[99] Cohenford, M. A., Rigas, B.A., *Proc. Natl. Acad. Sci*, *USA*, 1998, **95,** 15327-15332

[100] Schubert, J. M., Bird, B., Papamarkakis, K., Miljković, M., Bedrossian, K., Laver, N., Diem, M., *Lab. Invest.*, 2010, **90**, 1068-1077

[101] Boydston-White, S., Gopen, T., Houser, S., Bargonetti, J., Diem, M., *Biospectroscopy*, 1999,

[102] Jimenez-Hernandez, M., Hughes, C., Bassan, P., Ball, F., Brown, M. D., Clarke, N. W., Gardner, P., *Analyst*, 2013, **138**, 3957-3966

[103] Bassan, P., Byrne, H. J., Bonnier, F., Lee., J., Dumas, P., Gardner, P., *Analyst*, 2009, **134**, 1586-1593

[104] Romeo, M., Mohlenhoff, B., Diem, M., *Vib. Spectroscopy*, 2006, **42**, 9-14

[105] Flower, K. R., Khalifa, I., Bassan, P., Demoulin, D., Jackson, F., Lockyer, N. P., McGown, A. T., Miles, P., Vaccari, L., Gardner, P., *Analyst*, 2011, **136**, 498

[106] Hughes, C., Liew, M., Sachdeva, A., Bassan, P., Dumas, P., Hart, C. A., Brown, M. D., Clarke, N. W., Gardner, P., *Analyst*, 2010, **135**, 3133

[107] Clemens, G., Flower, K. R., Henderson, A. P., Whiting, A., Przyborski, S. A., Jimenez-Hernandez, M., Ball, Bassan, P., Cinque, G., Gardner, P., *Mol. Biosyst.*, 2013, **9**(4), 677-692

[108] Clemens, G., Flower, Gardner, P., Henderson, A. P., Knowles, J. P., Marder, T. B., Whiting, A., Przyborski, S. A., *Mol. Biosyst*., 2013, **9**(12), 3124-3134

[109] Gazi, E., Dwyer, J., Gardner, P., Ghanbari-Siahkali, A., Wade, A., Miyan, J., Lockyer, N., Vickerman, J., Clarke, N., Shanks, J., Scott, L., Hart, C., Brow,n M., *J. Pathol.*, 2003, **201**, 99-108

[110] Bird, B., Romeo, M. J., Diem, M., Bedrossian, K., Laver, N., Naber, S., *Vib. Spec.*, 2008, **48**, 101-106

[111] Pijanka, J., Sockalingum, G. D., Kohler, A., Yang, Y., Draux, F., Parkes, G., Lam, K. P., Collins, D., Dumas, P., Sandt, C., van Pittius, D. G., Douce, G., Manfait, M., Untereiner, V., Sulé-Suso, J,. *Lab Invest*, 2010, **90**, 797-807

[112] Walsh, M. J., Singh, M. N., Stringfellow, H. F., Pollock, H. M., Hammiche, A., Grude, O., Fullwood, N. J., Pitt, M. A., Martin-Hirsch, P. L., Martin, F. L., *Biomark Insights*, 2008, **3**, 179-189

[113] Sindhuphak, R., Issaravanich, S., Udomprasertgu,l V., Srisookho, P., Warakamin, S., Sindhuphak, S., Boonbundarlchai, R., Dusitsin, N., *Gyn. Oncol*., 2003, **90**, 10–14

[114] El-Tawil, S. G., Adnan, R., Muhamed, Z. N., Othman, N. H., *Pathology*, 2008, **40**, Conf Proc IEEE Eng Med Biol Soc., 600-3

[115] Njoroge, E., Alty, S. R., Gani, M. R., Alkatib, M., 2006, *Conf Proc IEEE Eng Med Biol Soc*., **1**:5338-41

[116] Jusman, Y., Sulaiman, S. N., Isa, N. A. M., Yusoff, I. A. Adnan, R., Othman, N. H., Zaki, A., *IEEE*, 2009, *TENCON 2009 IEEE Region 10 Conference*, 1-6, doi: 10.1109/TENCON.2009.5396006

[117] Yessi, J., Mat Isa, N. A., Adnan, R., Nor, H. O., *Ain Shams Engineering Journal*, **3**, 2012, 61–70.

[118] Kelly, J. G., Angelov, P. P., Walsh, M. J., Pollock, H. M., Pitt, M. A., Martin-Hirsch, P. L., Martin, F. L., *Int. J. Comp. Intell. Res.,* 2008, **4**, 392-401

[119] Ostrowska, K.M., Garcia, A., Meade, A.D., Malkin, A., Okewumi, I., O'Leary, J. J., Martin, C., Byrne, H. J., Lyng, F. M., *Analyst*, 2011, **136**, 1365-73

[120] Mostaco-Guidolin, L. B., Bachmann, L., *Appl. Spectrosc. Rev.*, 2011, **46(5),** 388-404

[121] Lee-Montiel, F. T., Reynolds, K. A., Riley, M. R., *J. Biomed. Eng.,* 2011, **5:16**

[122] Didonna, A., Vaccari, L., Bek, A., Legname, G., *ACS Chem Neurosci*., 2011, **2**, 160-74

[123] Mostaço-Guidolin, L. B., Murakami, L. S., Batistuti, M. R., Nomizo, A., Bachmann, L., *Spectroscopy*, 2010, **24**, 501-510

[124] Hughes, C., Liew, M., Sachdeva, A., Bassan, P., Dumas, P., Hart, C A., Brown, M. D., Clarke, N. W., Gardner, P., *Analyst.* 2010, **135**, 3133-3141

[125] American Cancer Society (www.cancer.org). Accessed on 28th March 2014

[126] Sulé-Suso, J.**,** Skingsley, D., Sockalingum, G. D., Kohler, A., Kegelaer, G., Manfait, M., El Haj, A. J., *Vib. Spec*, 2005, **38**, 179-184

[127] Draux, F., Jeannesson, P., Gobinet, C., Sule-Suso, J., Pijanka, J., Sandt, C., Dumas, P., Manfait, M., Sockalingum, G. D., *Anal. Bioanal. Chem.*, 2009, **395**, 2293-2301

[128] Derenne, A., Van Hemelryck, V., Lamoral-Theys, D., Kiss, R., Goormaghtigh, E., *Biochim Biophys Acta.*, 2013, **1832**, 46–56

[129] Gasper, R., Dewelle, J., Kiss, R., Mijatovic, T., Goormaghtigh E., *Biochim Biophys Acta,.* 2009, **1788**, 1263-1270

[130] Gasper, R., Mijatovic, T., Bénard , A, Derenne, A., Kiss, R., Goormaghtigh, E. Biochim Biophys Acta., 2010, **1802**, 1087-94.

[131] Bi, X., Walsh, M.J. , Wei, X., Sheng, G., Fu, J., Martin-Hirsch, PL., Thomas, G.O., Jones, K.C., Martin, F.L., *Environ. Sci. Technol.,* 2007, **41**, 5915-5922

[132] Ahmad, M.S., Mirza, B., Hussain, M., Hanif, M., Ali, S., Walsh, M.J., Martin, F.L.. *PMC Biophysics*, 2008, **5,** 1:3

[133] Llabjani, V., Jones, K.C., Thomas, G.O., Walker LA., Shore, R.F., Martin, F. L, *Environ. Sci. Technol.* 2009, **43**, 3356–3364

[134] Ukpebor, J., Llabjani, V., Martin, F.L., Halsall CJ, *Environ Toxicol Chem*. , **30**, 632–639, [177] Llabjani V, Trevisan J, Jones KC, Shore RF, Martin FL, Environ. Sci. Technol. 2011, 45, 6129–6135

[135] Llabjani, V., Trevisan, J., Jones, K. C., Shore, R. F., Martin, F. L., *Environ. Sci. Technol*., 2011, **45**, 6129-6135

[136] Pang, W., L, J, Ahmadzai, A.A., Heppenstall, L.D., Llabjani, V., Trevisan, J., Qiu, X., Martin, F.L. *Toxicology*, 2012, **298**, 24– 29.

[137] Dorling, K.M., Baker, M.J, *Trends Biotechnol*. 2013, **34**:437-438

[138] Filik, J., Rutter, A.V., Sulé-Suso, J., Cinque, G., *Analyst*, 2012, **137**, 5723-5239

[139] Vaccari, L., Birarda, G., Businaro, L., Pacor, S., Grenci, G., *Anal. Chem*., 2012, **84**, 4768-4775

[140] Whelan, D.R., Bambery, K.R., Heraud, P., Tobin, M.J., Diem, M., McNaughton, D., Wood, B.R., *Nucl. Acids Res*., 2011, 39, 5439-5848

[141] Mourant, J. R., Gibson R. R., Johnson, T. M., Carpenter, S., Short, K. W., Yamada, Y. R., Freyer, J. P., *Phys. Med. Biol*. 2003, **48**, 243-257

[142] Holman, H. N., Bechtel, H. A., Hao, Z., Martin, M. C., *Anal. Chem.*, 2010, **82**, 8757-8765

[143] Quaroni, L., Zlateva, T., Normand, E., *Anal. Chem.*, 2008, **83(19)**, 7371-7380

[144] Vaccari, L., Birarda, G., Grenci, G. Pacor, S., Businaro, L., *J. Phys.: Conf. Ser.*, 2012, **359**

[145] Birarda, G., Grenci, G., Businaro, L., Marmiroli, B., Pacor, S., Vaccari, L,*Microelectronic engineering*, 2010, **87,** 806-809

[146] Giovanni Birarda, Gianluca Grenci, Luca Businaro, Benedetta Marmiroli, Sabrina Pacor, Federica Piccirilli, Lisa Vaccari, *Vibrational Spectroscopy*, 2010, **53 (1)**,6–11

[147] Mattson, E. C., Aboualizadeh, E., Barabas, M. E., Stucky, C, Hirschmugl, C. J., *Int. J. Mol. Sci.* 2013, **14**, 22753-22781

[148] Nasse, M.J.; Ratti, S.; Giordano, M.; Hirschmugl, C.J. Appl. Spectrosc. 2009, **63**, 1181–1186

[149] Tobin, M. J., Puskar, L., Barber, R. L., Harvey, E. C., Heraud, P., Wood, B. R., Bambery, K. R., Dillon, C. T., Munro, K. L. *Vib. Spectrosc*., 2010, **53**, 34–38

[150] Holman, H. Y. N., Miles, R., Hao, Z., Wozei, E., Anderson, L. M., Yang, H., *Anal. Chem.* 2009, **81**, 8564–8570

[151] Whelan, D. R., Bambery, K. R., Puskar, L., McNaughton, D., Wood, B. R., *Analyst*, 2013, **138**, 3891-3899

[152] Yao, S., Moenner, M., Engdahl, A., Petibois, C., *Anal. Bioanal. Chem*., 2012, **404**, 1311-1316

[153] Soh, J., Chueng, A., Adio, A., Cooper, A. J., Birch, B.R., Lwaleed, B.A., *J. Clin. Pathol*. 2013, **66**, 312-318

[154] Petibois, C., Piccinini, M., Guidi, M. C., Marcelli, A. J., *Synchrotron Radiat*. 2010, **17,** 1–11

[155] Hirschmugl, C. J., Gough, K. M., *Appl. Spectrosc*. 2010, **66**, 475-491

[156] Chan KL, Kazarian SG, Analyst. 2013, **138**, 4040-7

[157] Chan, K. L., Kazarian, S. G., *Anal. Chem.*, 2013, **85**, 1029-1036

[158] Kazarian, S.G., Chan, K.L., *Analyst*, 2013, **138**, 1940

[159] Khoshmanesh, A., Dixon, M. W. A., Kenny, S., Tilley, L., McNaughton, D., Wood, B. R., *Anal. Chem*., 2014, **86**, 4379-4386

[160] Puppels, G. J., de Mul, F. F. M., Otto, C., Greve, J., Robert-Nicoud, M., Arndt-Jovin, D. J., Jovin, T. M., *Nature*, 1990, **347**, 301-303

[161] Puppels, G. J., Garritsen, H. S., Segers-Nolten, G. M., de Mul, F. F. M., Greve, C., *Biophys. J.*, 1991, **60**, 1046-1056

[162] Chan, J. W., Taylor, D. S., Zwerdling, T., Lane, S. M., Ihara, K., Huser, T., *Biophys. J.*, **90**, (2006), 648-656

[163] Jess, P. R., Smith, D. D., Mazilu, M., Dholakia, K., Riches, A. C., Herrington, C.S,. *Int. J. Cancer*., 2007, **15**, 2723-2728

[164] Krafft, C., Knetschke, T., Fyunk, R. H., Salzer, R., *Anal. Chem*., 2006, **78**

[165] Oshima, Y., Shinzawa, H., Takenaka, T., Furihata, C., Sato, H., *J.Biomed. Opt*., 2010, **15**, 017009

[166] Muratore, M., *Anal. Chem. Acta.,* 2013, **793**:1-10

[167] Matthews, Q., Jirasek, A., Lum, J., Duan, X., Brolo, A. G., *Appl. Spectro.*, 2010, **64**, 871-887

[168] Swain, R. J., Jell, G., Stevens, M. J., *J. Cell. Biochem.,* 2008, **104**, 1427-1438

[169] Pyrgiotakis, G., Kundakcioglu, E., Finton, K., Pardalous, P. M., Powers, K., Moudgil, B. M., *Ann. Biomed. Eng.*, 2009, **37**

[170] Verrier, S., Notingher, I., Polak, J. M., Hench, L. L., *Biopolymers*, 2004, **74**, 157–162

[171] Chan, J., Fore, S., Wachsmann-Hogiu, S., Huser, T. *Laser & Photon. Rev.*, 2008, **2**, 325–349

[172] Zheng, F., Qin, Y., Chen, K., *J. Biomed. Opt.*, 2007, **12**, 034002

[173] Konorov, S. O., Jardon, M. A., Piret, J. M., Blades, M. W., Turner, R. F. B., *Analyst*, 2012, **137**, 708-715

[174] Lin, H-H., Li, Y-C., Chang, C-H., Liu, C., Yu, A. L., Chen, C-H., *Anal. Chem.,* 2012, **84**, 113-120

[175] Buckmaster, R., Asphahani, F., Thein, M., Xu, J., Zhang, M., *Analyst*, 2009, **134**, 1440-1446

[176] Bonnier, F., Petitjean, F., Baker, M.J., Byrne, H.J., *J. Biophotonics*, 2014, **7**, 167-179

[177] Bonnier, F., Mehmood, A., Knief, P., Meade, A.D., Hornebeck, W., Lambkin H., Flynn, K., McDonagh, V., Healy, C., Lee, T.C., Lyng, F.M., Byrne, H.J., *J. Raman Spec.*, 2011, **42**, 888-896

[178] Bonnier, F., Knief, P., Lim, B., Meade, A.D., Dorney, J., Bhattacharya, K., Lyng, F.M., Byrne, H., *Analyst*, 2010, **135,** 3169-3177

[179] Palonpon, A. F., Sodeoka, M., Fujita, K., *Curr. Opin. Chem. Biol.*, 2013, **17**, 708-715

[180] Klein, K., Gigler, A. M., Aschenbrenner, T., Monetti, R., Bunk, W., Jamitzky, F., Morfill, G., Stark, R. W., Schlegel, J., *Biophys. J.*, 2012, **102**, 360-368

[181] Krafft, C., Knetschke, T., Siegner, A., Funk, R. H. W., Salzer, R., *Vib. Spectro*., 2003, **32**, 75-83

[182] Scalfi-Happ, C., Jauss, A., Ibach, W., Hollricher, O., Fulds, S., Hauser, C., Steiner, R., Rück, A., *Med. Laser App.*, 2007, **22**, 157-164

[183] Seydou, Y., Chen, H.H., Harte, E., Della Ventura, G., Petibois, C., *Anal. Bioanal. Chem.*, 2013, **405**, 8701-8707

[184] Majzner, K., Kaczor, Kachamakova-Trojanowska, N., Fedorowicz, A., Chlopicki, S., Baranska, M., *Analyst*, 2013, **138**, 603-610

[185] Lau, K., Berquand, A., Shorrocks, A. J., Baker, M. J., *Biomed. Spec. Imag.*, 2014, In Press. DOI 10.3233/BSI-140071

[186] Pallaoro, A., Hoonejani, M. R., Braun, G. B., Meinhart, C., Moskovits, M., *J. Nanophoton.*, 2013, **7**, 073092-073092

[187] Pallaoro, A., Braun, G. B., Moskovits, M., *Proc. Natl. Acad. Sci. USA.,* 2011, **108**, 16559-16564

[188] Chourpa, I., Lei, F.H., Dubois, P., Manfait, M., Sockalingum, G.D., *Chem. Soc. Rev.*, 2008, **37**, 993-1000

[189] Kneipp, J., Kneipp, H., Wittig, B., Kneipp, K., *Nanomedicine: Nanotechnology, Biology and Medicine*, 2010, **6**, 214-226

[190] Kneipp, J., Kneipp, H., Rajadurai, A., Redmond, R.W., Kneipp, K., *Journal of Raman Spectroscopy*, 2009, **40**, 1-5

[191] Vo-Dinh, T., Kasili, P., Wabuyele, M., *Nanomedicine: Nanotechnology, Biology and Medicine*, 2006, **2,** 22-30

[192] Hodges, M.D, Kelly, J.G., Bentley, A.J., Fogarty, S., Patel, I.I, Martin, F.L., Fullwood, N.J., *ACS Nano,* 2011, **12**, 9535-9541

[193] Bohme, R., Richter, M., Cialla, D., Rosch, P., Deckert, V., Popp, J., *J. Raman. Spectro*., 2009, **40**, 1452-1457

[194] Budich, C., Neugebauer, U., Popp, J., Deckert, V., *J. Microsc.*, 2007, **229**, 533-539

[195] Ashkin, A., *Phys. Rev. Lett.,* 1970, **24**, 156-159

[196] Snook, R. D., Harvey, T. J., Faria, E. C., Gardner, P., *Integr. Biol.*, 2009, **1**, 43-52

[197] Bankapur, A., Zachariah, E., Chidangil, S., Valiathan, M., Mathur, D., *PLoS ONE*, 2010, **5**, doi:10.1371/journal.pone.0010427

[198] Chan, J. W., Taylor, D. S., Lane, S. M., Zwerdling, T., Tuscano, J., Huser, T., *Anal. Chem.*, 2008, **80**, 2180-2187

[199] Harvey, T. J., Hughes, C., Ward, A. D., Faria, E. C., Henderson, A., Clarke, N. W., Brown, M. D., Snook, R. D., Gardner, P., *J. Biophotonics*, 2009, **2**, 47-49

[200] Dochow, S., Krafft, C., Neugebauer, U., Bocklitz, T., Henkel, T., Mayer, G., Albert, J., Popp, J., *Lap Chip*, 2011, **11**, 1484-1490

[201] Hamden, K. E., Bryan, B. A., Ford, P. W., Xie, C., Li, Y. Q., Akula, S. M., *J. Virol. Methods*., 2005, **129**, 145-151

[202] Deng, J. L., Wei, Q., Zhang, M. H., Wang, Y. Z., Li, Y. Q., *J. Raman. Spectrosc.*, 2005, **36**, 257-261

[203] Lau, A. Y., Lee. L. P., Chan, J. W., *Lab Chip*., 2008, **8**, 1116-1120.

[204] Li, M., Xu, J., Romero-Gonzalez, M., Banwart, S. A., Huang, W. E., *Curr. Opin. Biotechnol.,* 2012, **23**, 56-63

[205] Dochow, S., Beleites, C., Henkel, T., Mayer, G., Albert, J., Clement, J., Krafft, C., Popp, J., *Anal. Bioanal. Chem.*, 2013, **405**, 2743-2746

[206] Camp, C, H., Yegnanarayanan, S., Eftekhar, A. A., Hamsa, S., Adibi, A., *Opt. Express*., 2009, **17**, 22889-22889

[207] Pascut, F. C., Goh, H. T., George, V., Denning, C., Notingher, I., *J. Biomed. Opt.,* 2011, **16**, 045002

[208] Garrett, N., Whiteman, M., Moger, J., *Optics Express*, 2011, **19(18)**,17653-17574

[209] Zhang, X., Roeffaers, M. B. J., Basu, S., Daniele, J. R., Fu, D., Freudiger, C. W., Holtom, G. R., Xie, X. S., *Chem. Phys. Chem.*, 2012, **13**, 1054-1059

[210] Amrania, H., McCrow, A. P., Matthews, M. R., Kazarian, S. G., Kuiminova, M. K., Phillips, C. C., *Chem. Sci.*, 2011, **2**, 107

[211] Evans, M.J., Clemens, G., Casey, C., Baker, M.J., *Vib. Spec.*, 2014, **72**, 37-43

[212] Maquelin, K., Kirschner, C., Choo-Smith, L.-P., van den Braak, N., Endtz, Ph. H., Naumann, D., Puppels, G.J.J., *Microbiol. Methods.*, 2002, **51**, 255-271

[213] Pijanka, J.K., Stone, N., Rutter, A., Forsyth, N., Sockalingum, G.D., Yang., Sulé-Suso, Y., J., *Analyst*., 2013, **138**, 5052-5058

[214] Palonpon, A.F., Sodeoka, M., Fujita, K., *Curr. Opin. Chem. Biol.,*2013, **17**, 708-715

[215] Krafft, C., Knetschke, T., Siegne, A., Funk, R.H.W., Salzer, R., *Vib. Spectrosc*., 2003, **32**, 75-83

[216] Draux, F., Jeannesson, P., Beljebbar, A., Tfayli, A., Fourre, N., Manfait, M., Sulé-Suso, J., Sockalingum, G.D., *Analyst*., 2009, **134**, 542-548

[217] Huang, W.E., Lie, M., Jarvis, R.M., Goodacre, R., Banwart, S.A., in *Advances in Applied Microbiology*, Elsevier, Burlington: Academic Press, Vol. 70, 2010, 153-186

[218] Pijanka, J.K., Kumar, D., Dale, T., Yousef, I., Parkes, G., Untereiner, V., Yang, Y., Dumas, P., Collins, D., Manfait, M., Sockalingum, G.D., .Forsyth, N.R, Sulé-Suso, J., *Analyst*, 2010, **135**, 3126-3132

[219] Miller, L., Bourassa, M.W., Smith, R.J., *Biochim. Biophys. Acta*, 2013, **18220**, 2339-2346

[220] Mohlenhoff, B., Romeo, M., Diem, M., Wood, B.R., *Biophys. J.*, 2005, **88**, 3635-3640

[221] Pijanka, J.K., Kohler, A., Yang, Y., Dumas, P., Chio-Srichan, S., Manfait, M., Sockalingum, G.D., Sulé-Suso, J., *Analyst*, 2009, **134**, 1176-1181

[222] McIntosh, L.M., Jackson, M., Mantsch, H.H., Stranc, M.F., Pilavdzic, D., Crowson, A.N., *J. Invest. Dermatol.*, 1999, **112**, 951-956

[223] Pijanka, J., Sockalingum, G.D., Kohler, A., Yang, Y., Florence, D., Parkes, G., Lam, K., Collins, D., Duman, P., Sandt, C., van Pittius, D., Douce, G., Manfait, M., Untereiner, V., Sulé-Suso, J., *Lab. Invest.* 2010, **90**, 797-807

[224] Patel, I.I., Harrison, W.J., Kerns, J.G., Filik, J., Wehbe, K., Carmichael, P.L, Scott, A.D., Philpott, M.P., Frogley, M.D., Cinque, G., Martin, F.L., *Anal. Bioanal. Chem.*, 2012, **404**, 1745-1758

[225] Dougan, J.A., Kazarian, S.G., *Spectrosc. Eur.*, 2013, **25**, 6-12

[226] Amrania, H., McCrow, A.P., Matthews, M.R., Kazarian, S.G., Muimova, M.K., Phillips, C.C., *Chem. Sci,* 2011, **2**, 107-111

[227] Griffiths, P. R., de Haseth, J. A., *Fourier Transform Infrared Spectrometry*, John Wiley & Sons, Inc., Honoken, New Jersey, 2nd edn., 2007

[228] Sun, X., Xu, Y., Wu, J., Zhang, Y., Sun, K., *J. Surg. Res.*, 2013, **179**, 33-38

[229] Glassford, S.E., Byrne, B., Kazarian, S. G., *Biochim. Biophys. Acta*. , 2013, **1834**, 2849-2858

[230] Baker, M.J., Trevisan, J., Bassan, P., Bhargava, R., Butler, H., Dorling, K. M., Fielden, P. R., Fogarty, S. W., Fulwood, N. J., Heys, K., Hughes, C., Lasch, P., Martin-Hirsch, P. L.., Obinaju, B., Sockalingum, G. D., Sulé-Suso, J., Strong, R. J., Walsh, M. J., Wood, B. R., Gardner, P., Martin, F. L., *Nat. Protoc.*, 2014, In Press DOI: 10.1038/nprot.2014.110

[231] Kazarian, S. G., Andrew Chan, K. L., *Analyst*, 2013, **138**, 1940-1951

[232] Petibois, C., Cestelli-Guidi, M., Piccinini, M., Moenner, M., Marcelli, A., *Anal. Bioanal. Chem.*, 2010, **397**, 2123-2129

[233] Zhu, J., Zhou, J., Guo, J., Cai, W., Liu, B., Wang, Z., Sun, Z., *Chem. Cent. J.,* 2013, **7**, 37

[234] Abramczyk, H., Brozek-Pluska, B., Surmacki, J., Jablonska, J., Kordek, R., *J. Mol. Liq*., 2011, **164**, 123-131

[235] Zhang, Y., Hong, H., Cai, W., *Curr. Pharm. Biotechnol.,* 2010, **11**, 654-661

[236] McCreery, R. L., *Raman Spectroscopy for Chemical Analysis,* John Wiley & Sons, Inc. Honoken, New Jersey, 2005

[237] Everall, N., *J. Raman. Spectrosc.*, 2013, **45**, 133-138

[238] Majzner, K., Kaczor, A., Kachamakova-Trojanowska, N., Fedorowicz, A., Chlopicki, S., Baranska, M., *Analyst*, 2013, **138**, 603-610

[239] Seydou, Y., Chen, H., Harte, E., Ventura, G. D., Petibois, C., *Anal. Bioanal. Chem.*, 2013, **405**, 8701-8707

[240] Pahlow, S., März, A., Seise, B., Hartmann, K., Freitag, I., Kämmer, E., Böhme, R., Deckert, V., Weber, K., Cialla, D., Popp, J., *Eng. Life. Sci*, 2012, **12**, 131-143

[241] Schrojenstein Lantman, E. M., Deckert-Gaudig, T., Mank, A. J. G., Deckert, V., Weckhuysen, B. M, *Nature Nanotechnol*, 2012, **7**, 583-586

[242] Kurouski, D., Postiglione, T., Deckert-Gaudig, T., Deckert, V., Lednev, I. K, *Analyst*, **138**, 1665-1673

[243] Wright, A. J., Poland, P., Girkin, J. M., Freudiger, C. W., Evans, C. L., Xie, X. S., *Opt. Express*, 2007, **15**, 18209-18219

[244] Ganikhanov, F., Carrasco, S., Xie, X. S., *Opt. Lett.,* 2006, **31**, 1292-1294

[245] Potma, E. O., Xie, X. S., Mutean, L., Preusser, J., Jones, D., Ye, D., Leone, S. R., Hinsberg, W. D., Schade, W., *J. Phys. Chem.*, 2004, **108**, 1296-1301

[246] Evans, C. L., Potma, E. O., Puoris'haag, M., Cộtē, D., Lin, C. P., Xie, X. S., *Proc. Natl. Acad. Sci. U.S.A.,* 2005, **102**, 16807-16812

[247] Fu, D., Holtom, G., Freuiger, C., Zhang, X., Xie, X. S., *J. Phys. Chem.*, 2013, **117**, 4634-4640

[248] Lu, F., Ji, M., Fu, D., Ni, X., Freudiger, C. W., Holtom, G., Xie, X. S., *Mol. Phys.*, 2012, **110**, 1927-1932

[249] Saar, B. G., Contreras-Rojas, L. R., Xie, X. S., Guy, R. H., *Mol. Pharm.*, 2011, **8**, 969-975

[250] Ji, M., Orringer, D. A., Freudiger, C. W., Ramkissoon, S., Liu, X., Lau, D., Golby, A. J., Norton, I., Hayashi, M., Agar, N. Y. R., Young, G. S., Spino, C., Santagata, S., Camelo-Piragua, S., Ligon, K. L., Sagher, O., Xie, X. S., *Sci. Transl. Med.*, 2013, **5**, 1-10

[251] Fu, D., Lu, F., Zhang, X., Freudiger, C., Pernik, D. R., Holtom, G., Zie, X. S., *J. Am. Chem. Soc.*, 2012, **134**, 3623-3626

[252] Quaroni, L., Zlateva, T., *Analyst*, 2011, **136**, 3219-3232

[253] Quaroni, L., Zlateva, T., Bedolla, D., Massaro, S., Torre, V., *Chem Phys Chem,* 2008, **9(10),** 1380-1382

[254] Quaroni, L., Zlateva, T., Sarafimov, B., Kreuzer, H.W., Wehbe, K., Hegg, E.L, Cinque, G., *Biophys. Chem.*, 2014, **189**, 40-48.

Figure Legends

Figure 1. Results of bibliometric analysis of the number of citations per year listed on ISI Thomson Web of Science ® (http://wok.mimas.ac.uk) for the period of 1986 – 2013, using the search terms (A) Raman and Cytology, (B) FTIR and Cytology, (C) Raman Imaging and Cytology and (D) FTIR Imaging and Cytology

Figure 2 (A) Bright-filed microscopic image of a *B.cereus* cell population (B) Raman image using the integrated Raman intensity of the ν(C=O) stretching vibration at 1726 cm^{-1} (blue-PHB), of the C-H stretching intensities in the 2800-3000 cm^{-1} (red-cell) and of the symmetric ring 'breathing' of pyridine at 1018 cm^{-1} (green-spore) of the area shown in A. (C) Corresponding Raman average spectra of the chemical image B. Reproduced from Hermelink *et al.* [58]

Figure 3. Stacked SERS spectra showing the spectra obtained from the simultaneous detection of all three bacterial meningitis pathogens using the detection assay (a) and the SERS spectra obtained from each pathogen separately: *N. meningitides* (b), *H. influenza* (c), and *S. pneumonia* (d). SERS spectra were recorded using an excitation wavelength of 532 nm and a diode laser with a 10 s accumulation time. Dotted red lines show peaks that are unique to each SERS spectrum and hence the pathogen. Reproduced from Gracie *et al.* [62].

Figure 4. Visual images (A–D) and average absorbance FTIR chemical maps (E–H) representing cells present in the investigated samples. (A and E) C33A cell, (B and F) SiHa cells, (C and G) HeLa cells, (D and H) CaSki cells. Red colour represents region of a nucleus, green and light blue—region of a cytoplasm, violet—background. [119].

Figure 5 Location and separation of individual cell regions (a) white-light reflection image of CALU-1 cells, (b) IR absorbance image of the same sample area, (c) same image as (b) but gray scale, regional maxima shown as red markers, (d) cell separation lines calculated by watershed transform (cell-to-background borders not shown) and (e) separated cell regions, each cell shown as a different colour, background black, separation lines and rejected regions white [138].

Figure 6 (a) Schematic diagrams showing the procedure of seeding live cells on a removable ATR sliding plate (left) and how it is attached to the objective during measurement (right). (b) Photograph of the actual ATR sliding plate (left) and when it is integrated to the ATR objective (right). (c) FTIR images (left) generated using different spectral bands and the extracted spectra (right), after the subtraction of absorbance of water, from locations indicated on the FTIR image generated using the 1085 cm^{-1} band [159].

Figure 7. Single cell U-87MG malignant grade IV glioblastoma cell line. a) White light image. The box outlines the volume imaged area b) AFM 3D-rendering topographical image c) Young's modulus (YM) score image of the cells. The colour bar illustrates the YM of the sample in MPa d) composite principal component spectral image of the cell (grey) and quartz substrates (magenta) e) spectral information showing peaks responsible for cellular information f)Principal Component Analysis image showing the nucleus in red and membrane bound organelles in blue g) peaks explaining the chemistry of the subcellular structure. Reproduced from reference [186].

Table Legends

Table 1. Tentative spectral assignments for Raman cellular spectra.

Table 2. Tentative spectral assignments for FTIR cellular spectra.

Table 3. Brief introduction to the specifics of each technique described in this review

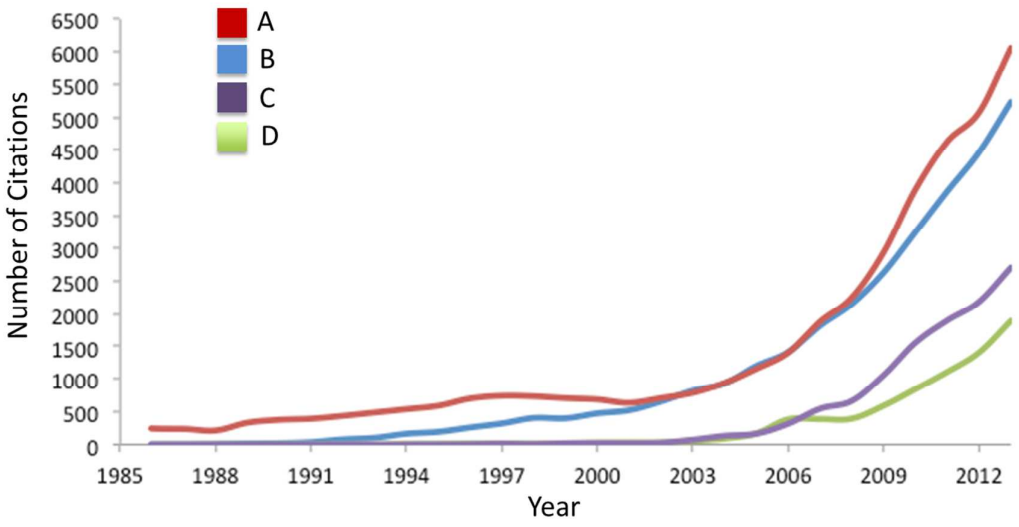

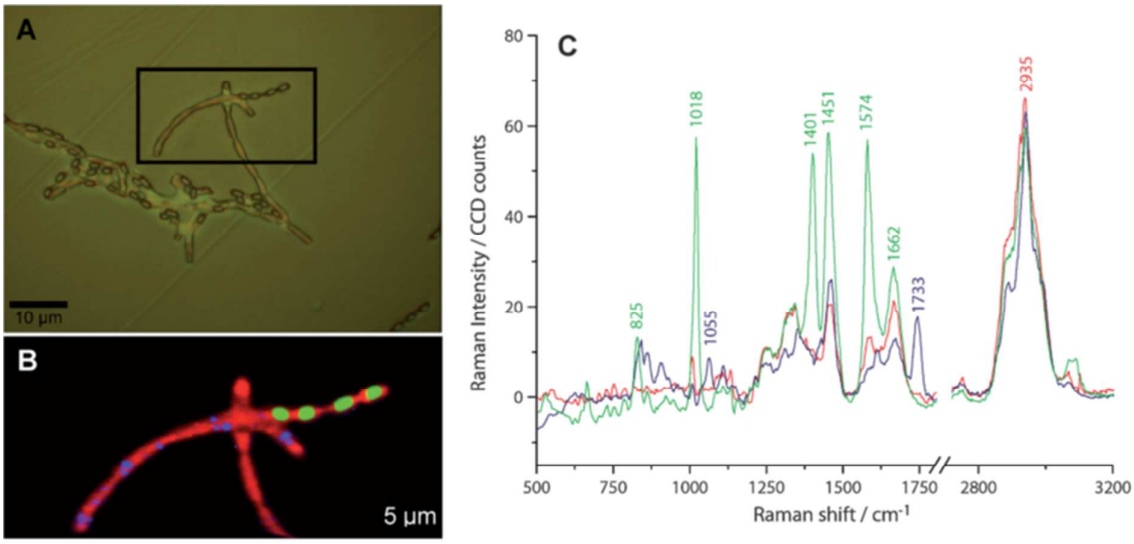

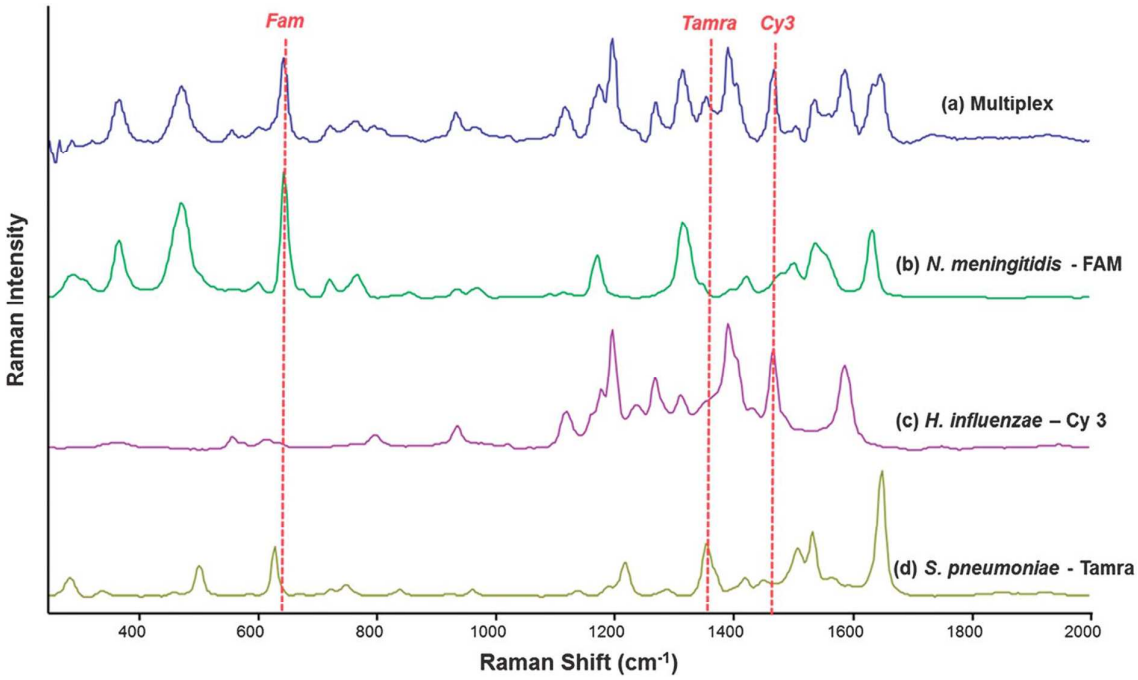

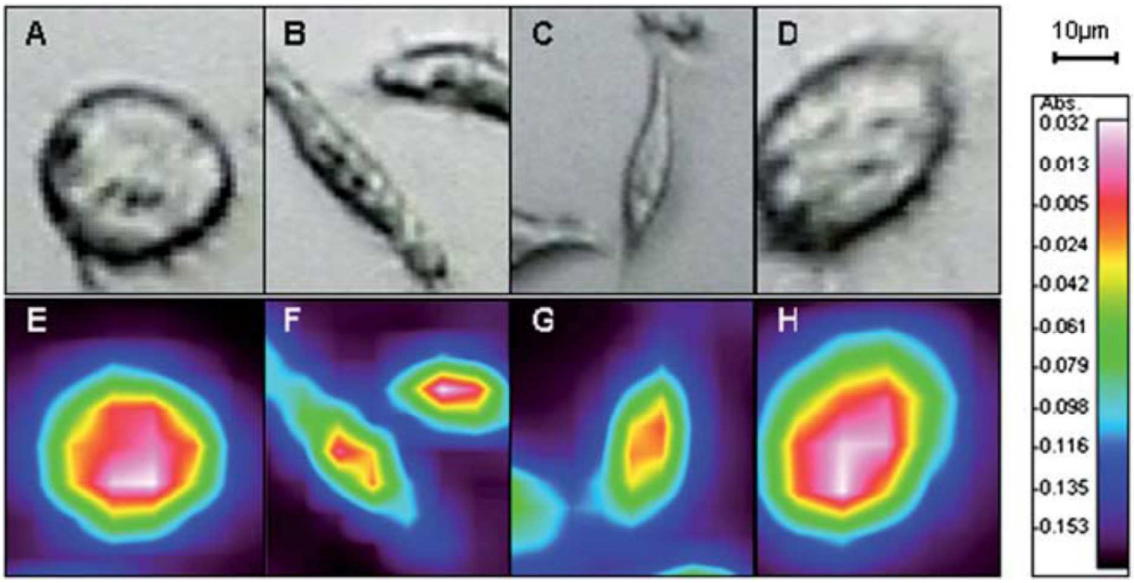

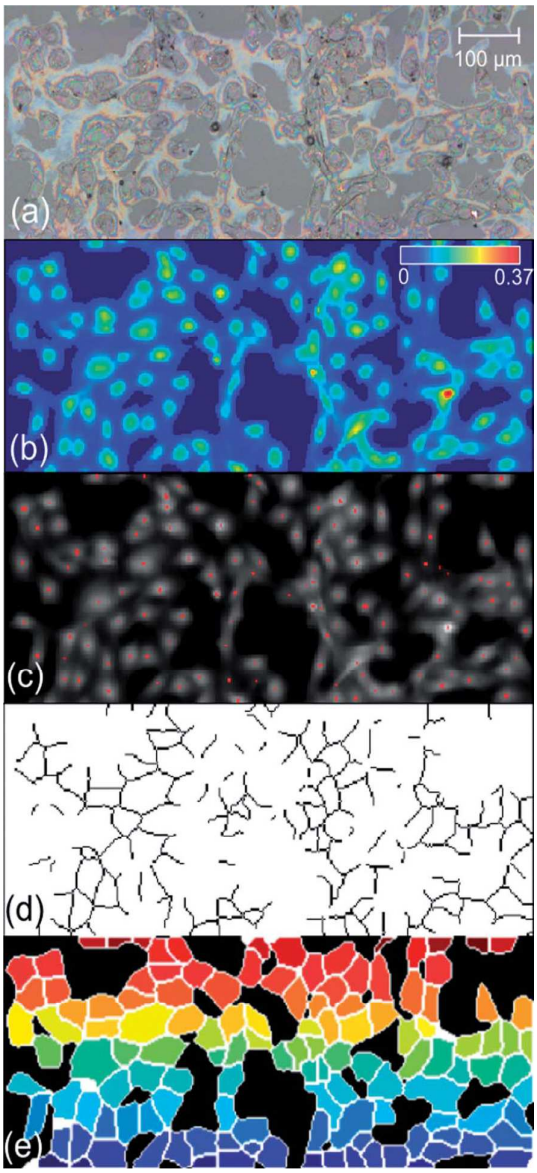

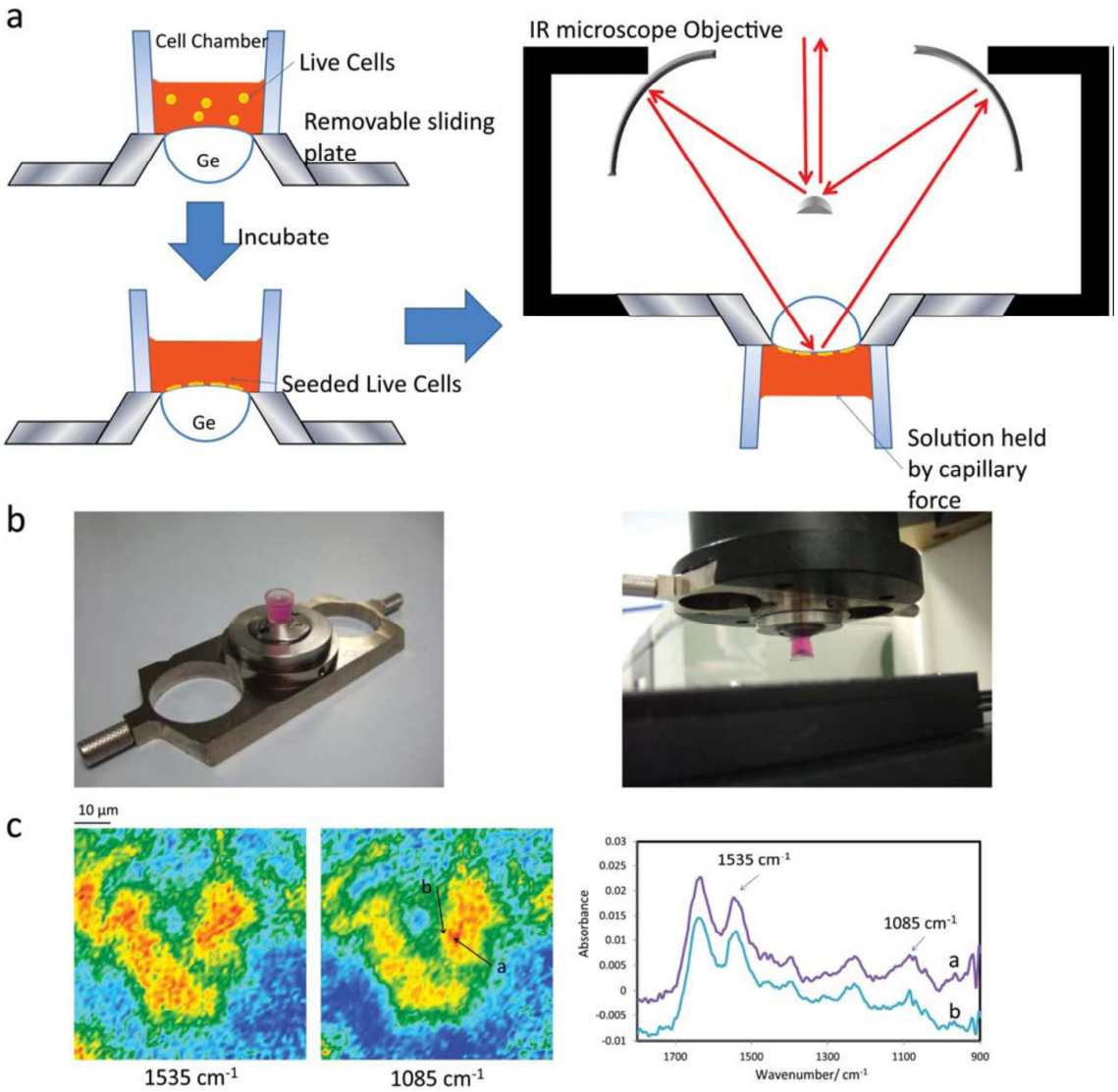

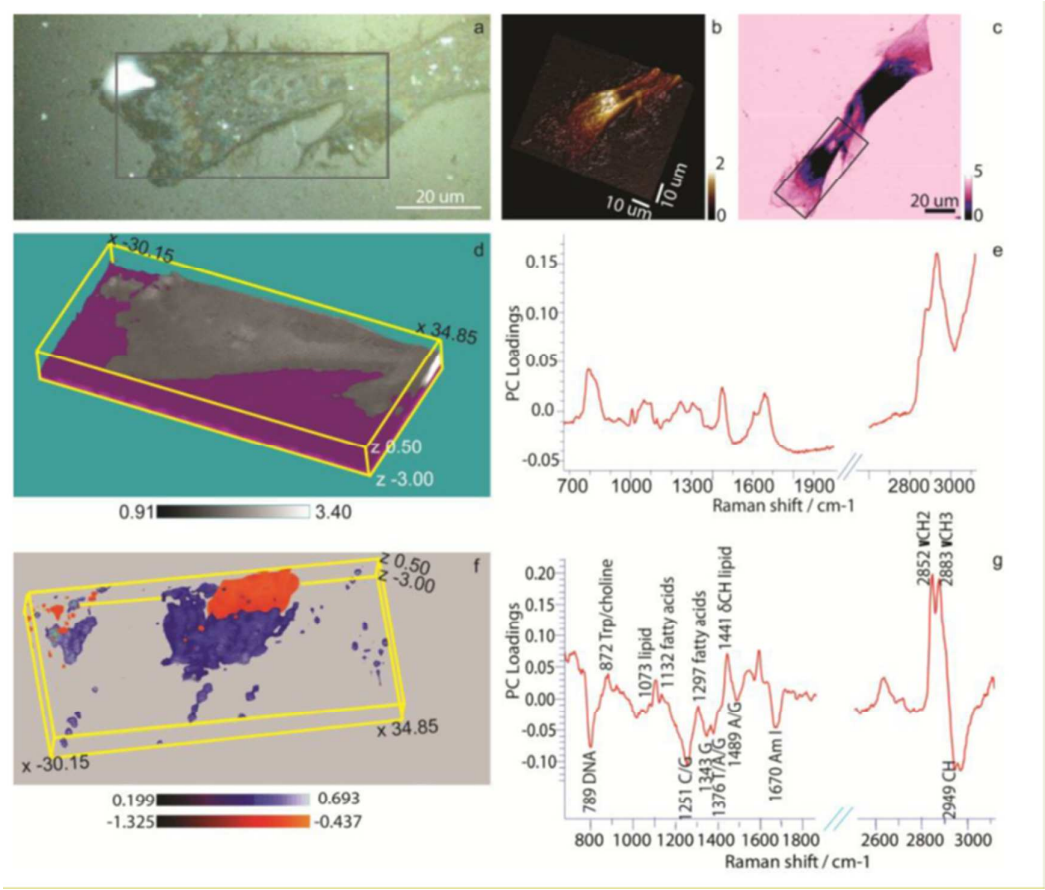

Raman

Frequency (cm^{-1})	Assignment
508-540	S-S stretch [212]
540	COC glycosidic ring deformation [212]
620	Phenylalanine [212]
640	Tyrosine [212]
665	Guanine [212]
702	Cholesterol [212]
719	Choline $(H_3C)N^+$ [212]
720	Adenine [212]
750	Cytochrome c (localised in mitochondria for ATP production) [215]
780	Cytosine, Uracil [212]
813-816	O-P-O stretch (DNA backbone) [13, 213, 214]
829-852	Tyrosine [212]
858	C-C stretch [212]
891-908	CH_3 rocking (fatty acid chain) [212]
914-925	C-O and C-C stretching (Ribose-phosphate) [212]
930-950	N-C and C-C stretches [212]
1004	Phenylalanine [212]
1025, 1047, 1155	C-O stretch (glycogen) [212]
1061	C-N and C-C stretches [212]
1085	C-O stretch [212]
1080	PO_2^- DNA symmetric stretch [13, 213, 214]
1098	C-C and COC stretches (glycosidic link) [212]
1174, 1325, 1370	Guanine ring stretches [13, 216]
1129	C-N and C-C stretches [13]
1135, 1235, 1395	Uracil ring stretches [216]
1235-1259	N-H and C-H (Amide III/β-sheet) [216]
1245, 1275	Cytosine ring stretches [13, 216]
1256, 1514	Adenine ring stretches [13, 216]
1260	N-H and C-H band (Amide III/distorted) [214]
1300-1340	N-H and C-H band (Amide III/α-helix) [214]
1440-1460	C-H_2 deformation [212]
1575	Adenine, guanine (ring structure) [212, 213]
1606	Phenylalanine [212]
1650-1660	Amide I/α-helix [13, 212]
1670-1680	Amide I/ β-sheet [13, 212]
1735	C=O ester stretch (thymine) [212]
2870-2890	CH_2 symmetric stretch [13, 214]
2935	CH_3 and CH_2 stretches [212]
2975	CH_3 stretch [212]
3059	(C=C-H) aromatic stretch [212]
3240	Water [217]

FTIR

Frequency (cm^{-1})	Assignment
600-900	"fingerprint region" [212]
980, 1080, 1240	Phosphate groups of nucleic acids [222]
720	C-H rocking of $>CH_2$ [212]
1023-1040	Glycogen [224, 225]
1035-1085	P=O symmetric/antisymmetric stretches of PO_2^- in nucleus [212, 220, 221, 224, 225]
900-1200	C-O-C, C-C stretch, C-O-H, C-O-C deformations of carbohydrates [212]
1220-1250	P=O asymmetric stretch of PO_2^- phosphodiesters [212]
1240-1310	Amide II band of protein [212, 226]
1400	C=O symmetric stretch of COO^- [212]
1455-1470	CH_2 and CH_3 deformations [212]
1515	Tyrosine band [212]
1520-1550	Amide II [212, 221, 224, 225]
1637	Amide I of β-sheet structures [212]
1655	Amide I of α-helical structures/C=O stretching [212, 219, 221]
1675, 1688, 1695	Amide I band (antiparallel pleated sheets and β-turns of proteins) [212]
1680-1715	C=O in nucleic acids [212]
1715	C=O stretch of carbonic acid [212]
1740	C=O stretch of esters [212, 218, 222]
22050	C-H symmetric stretch of CH_3 in fatty acids [212, 221, 223]
22070	C-H symmetric stretch of CH_3 [212]
22098	C-H stretch of C-H in methane groups in membrane lipids [212, 218, 221, 223]
22070-2960	CH_3 groups (lipids and nucleic acids) [212, 221]
2918	C-H antisymmetric stretch of CH_3 in fatty acid [214, 221]
2930	C-H antisymmetric stretch of CH_2 [212]
2955	C-H antisymmetric stretch of CH_3 in fatty acids [212]
3200	N-H stretch of proteins [212]
3500	O-H stretch of hydroxyl groups [212]

Technique	Brief Definition	References
Attenuated Total Reflection – Fourier Transform Infrared (ATR-FTIR)	ATR-FTIR is a sampling mode of FTIR whereby infrared light is directed at an interface between an infrared transparent material with a high refractive index (internal reflection element) and the sample of interest on the surface. The angle of incidence of the IR beam is greater than the critical angle, thus total internal reflection occurs. At the surface of the ATR crystal (ZnSe, Diamond, Si or Ge) an evanescent wave interacts with the sample. The depth at which the evanescent wave penetrates the sample is defined as the distance from the crystal-interface where the wave decays to 1/*e* - approximately 37 % - of its original value. ATR-FTIR is reagent-free and requires little or no sample preparation.	137, 227-229
FTIR Imaging	FTIR imaging is a fast and label-free technique which derives from the interaction of infrared light with the vibrational modes of the molecules being interrogated. As imaging is performed a spectrum from each point is acquired by raster scanning an illuminated point or by wide-field illumination and detecting the infrared light with either a focal plane array (FPA) or linear array detector. The three major imaging sampling modes are transmission, transflection and ATR, each mode offering advantages for some samples and challenges for others. FTIR imaging provides spatially-resolved information based on chemical specific spectra.	231-233
Surface Enhanced Raman Scattering (SERS)	SERS can provide local chemical composition of biomolecules at very low concentrations. It enormously enhances the Raman signal of a molecule in contrast to normal Raman by typically 10^3 to 10^6 when in close proximity/adsorption with a roughened metal surface, a colloidal solution or a roughened electrode. The enhancement is generated primarily by the strongly augmented electric field of the nanoparticle created by a surface plasma resonance and by a charge transfer mechanism (chemical enhancement). SERS has a fluorescence quenching effect and can achieve additional resonance enhancement (SERRS) by tuning to a specific chromophore.	13, 30, 234
Raman Imaging	Raman imaging utilises Raman scattered light to construct a two-dimensional image. Raman imaging is a label-free approach of collecting detailed chemical images (hyperspectral images) based on a sample's Raman spectrum with extremely high spatial resolution. The observed intensities are converted into a false colour image with spectra representative of each spatial location. The main imaging methods are; point-to-point profile, line imaging and "global" or "direct" imaging. Point-to-point imaging involves a sequence of single point acquisitions over user defined spatial locations. Line imaging focuses the Raman laser in a line. "Global" imaging involves illuminating a large sample area and collecting spatially resolved spectra. If the filter used passes through only a particular Raman shift to the CCD, then "global" imaging can result in a chemically selective two-dimensional image if the observed shift matches up with a specific sample component.	235-237
Confocal 3D Raman Imaging	Confocal 3D (three-dimensional) Raman imaging provides complex chemical information about various structures and is a non-destructive technique that can provide rapid analytical measurements. The 3D imaging offers high spatial resolution (lateral and depth) in the form of a 3D map in relatively short timescales. Raman 3D imaging has the potential to be used without labelling when identifying various organelles of a single cell, thus avoiding the generation of spectral artefacts. The collection of 2D images with high-resolution in a confocal-like mode can allow for 3D reconstructed images of cells or various samples due to the recent advances in Raman microscopy and fast acquisition detectors.	238-240
Tip Enhanced Raman Spectroscopy (TERS)	Tip-enhanced Raman spectroscopy is a nano-spectroscopic technique that combines the phenomenon of surface-enhanced Raman spectroscopy (SERS) with atomic force microscopy (AFM). Various tip designs has been reported to provide many ways for the reproducible and highly efficient placement of a single metallic particle on the apex of the tip. Typically, a thin coating of silver or gold on the AFM tip dramatically boosts the Raman signal via the excitation of surface Plasmon polaritons in a diameter of ≤ 10 nm around the tip. Unlike SERS, TERS allows for site-dependent, semi-quantitative conclusions to be drawn as the tip position is controlled relative to the sample and with high spatial resolution. Nanometre-scale resolution studies on biological samples (eukaryotic cells, bacteria, DNA etc.) depends largely on the TERS tip diameter.	241-243

Coherent anti-Stokes Raman Scattering (CARS)	Coherent anti-Stokes Raman scattering (CARS) is a non-linear optical technique that is sensitive to the Raman vibrational activity of the specimen of interest. CARS microscopy is a powerful, high-speed, label-free and non-invasive tool used for the chemical imaging of biological specimens with short acquisition times. CARS requires two laser frequencies called 'pump' (ωp) and 'Stokes' (ωS). When the frequency difference ω0 = ωp – ω_S (Raman shift) is tuned to the frequency of a Raman active molecular vibration, an enhanced anti-Stokes signal is generated at a frequency of $\omega_{AS} = 2\omega_p - \omega_S$. Due to the non-linear effect of CARS, the signal is only generated at the laser focus, this allows for point-by-point 3D imaging of thick biological specimens.	244-247
Stimulated Raman Scattering (SRS)	Stimulated Raman Scattering (SRS) microscopy has emerged as an alternative to CARS microscopy and unlike CARS; SRS is free from a non-resonant background and has straightforward image interpretation and quantification. Stimulated excitation of Raman scattering occurs, like CARS, when the difference in energy between two laser beams match that of a specific molecular vibration. SRS offers high-spatial resolution imaging of chemical distributions without the use of fluorescent labels. SRS signal is linearly proportional to the target molecule concentration and it has been reported that SRS has a video-rate imaging speed of 30 frames/s-1 with signal collection in reflective, thick and non-transparent samples. The combination of spectroscopic information and multicolour SRS microscopy allows for the differentiation of normal and tumour infiltrated tissues; SRS microscopy can detect tumour margins with label-free imaging. A major limitation of SRS is that only one single Raman band can be probed at any one time but the features of SRS make it a more desirable analytical tool compared to CARS.	248-251